

Supplementary information

Reusing wastewater for agricultural irrigation: a WEF Nexus assessment in the North Western Sahara Aquifer System

Camilo Ramirez ¹, Youssef Almulla ¹, and Francesco Fuso-Nerini ¹

¹ KTH Royal Institute of Technology, Stockholm, Sweden

E-mail: camilorg@kth.se

9 January 2021

Contents

1	Geographic Information Systems analysis	2
1.1	Land-cover and cropland area datasets	2
1.2	Population dataset	4
1.3	Depth to groundwater dataset	5
2	Data calibration	6
3	Domestic and irrigation water withdrawals	8
4	Groundwater pumping	8
5	Energy-for-wastewater	9
6	Wastewater Treatment System characteristics	9
7	Reverse Osmosis desalination	10
8	Levelised Cost of Water (LCOW)	13
9	Clusters	14
10	Water withdrawals and reuse per cluster	16
11	Energy demand per cluster	22
12	Least-cost technologies	25
13	Sensitivity analysis	28
13.1	Groundwater depth increase	28
13.2	TDS content	30
13.3	Irrigated area growth	33
13.4	Population growth and domestic water use	34
13.5	Discount rate.	39

1. Geographic Information Systems analysis

Geospatial characteristics of the NWSAS were obtained from open sources as described in table 1. All data layers were converted into matching units, re-projected into the Sud Algerie Degree projection (ESRI: 102592)—This projection was selected as it produces minimal distortions in the analysis area—, re-scaled to the same resolution and, when only individual data points were available, interpolated to extend the data to the entire analysed area (i.e. for the Groundwater quality layer). Furthermore, all layers were merged into a large data frame.

Table 1. Geographic Information System and statistical input datasets.

Layer	Coverage	Format	Resolution	Year	Source
Population	Algeria, Tunisia, Libya	raster (tif)	100 m grid cell	2015	[1]
Population	NWSAS	Tabular	Country share	2015	[2]
Depth to groundwater	Africa	txt table	5 km grid cell	2012	[3]
Administrative boundaries	Algeria, Tunisia, Libya	shapefile	Level 1 (provinces) polygons	2015	[4]
Transboundary aquifers borders	Global	shapefile	Individual polygons	2015	[5]
Groundwater quality	NWSAS Basin	data points	206 data points	2016	RA *
Land cover	Africa	raster (tif)	20 m grid cell	2016	[6]
Aquifer boundaries	NWSAS basin	shapefile	Individual polygons	-	RA *
Minimum temperature (°C)	Global	raster (tif)	30 arc second, monthly	1970-2000	[7]
Average temperature (°C)	Global	raster (tif)	30 arc second, monthly	1970-2000	[7]
Max temperature (°C)	Global	raster (tif)	30 arc second, monthly	1970-2000	[7]
Wind speed (m/s)	Global	raster (tif)	30 arc second, monthly	1970-2000	[7]
Solar irradiation (kJ/m ² day)	Global	raster (tif)	30 arc second, monthly	1970-2000	[7]
Irrigated area (ha)	NWSAS	Tabular	Country share	2012	[2]
Irrigated area (ha)	NWSAS	Tabular	Provincial	2012	[8]
Irrigation water (m ³ /ha)	NWSAS	Tabular	Provincial	2012	[8]

* Regional Authorities.

1.1. Land-cover and cropland area datasets

Figure 1 shows the land-cover dataset used for the region. This data was developed by the Land Cover project of the ESA Climate Change Initiative, and consist of a

20×20 m resolution raster for the entire continent of Africa [6]. It classifies land-cover into nine categories: (1) Trees cover area, (2) Shrubs cover area, (3) Grassland, (4) Cropland, (5) Vegetation aquatic or regularly flooded, (6) Lichen Mosses/Sparse vegetation, (7) Bare areas, (8) Built up areas, and (9) Open water.

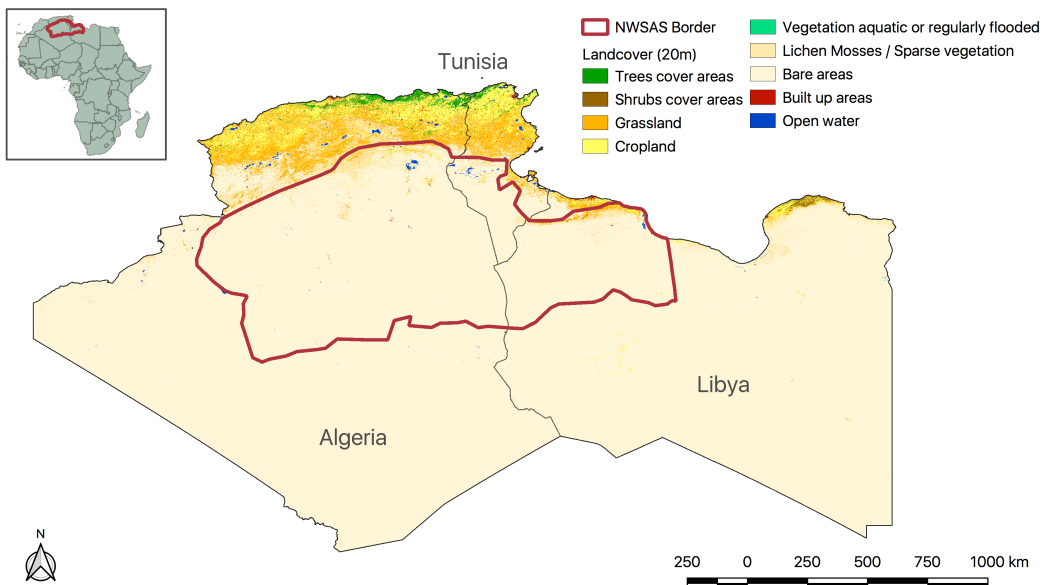


Figure 1. North Western Sahara Aquifer System - Land-cover map at 20×20 meters grid cell resolution.

From this dataset, some insights can already be obtained. Bare/desertic areas dominate the region, while open water bodies are quite uncommon, however, the water bodies found in the NWSAS region do not constitute “fresh water” resources due to their high content of salinity [9]. The built up areas are highly scattered throughout the NWSAS region as well as the cropland zones, which are mainly located in the surroundings of the built up areas and in the north of the region. The largest agricultural activity, is given at the north of the three countries, as well as the major urban concentrations, nonetheless, this does not make the NWSAS region less important, as the groundwater resources there, are crucial for ensuring food security for a growing population in the region.

From this land-cover dataset, the cropland areas were subtracted, allowing to create a raster layer containing the cropland density in the region. This layer was created for a resolution of 1km grid cell and calibrated for year 2015 according to regional statistics presented in Table 3. The obtained cropland dataset is showcased in Figure 2.

From Figure 2, it is depicted with more clarity that the main agricultural activity is in fact, presented in the northern region. The provinces with largest agricultural activity are: Biskra, El Oued, Ouargla, Adrar and Ghardaïa in Algeria; Kebili and Tozeur in Tunisia; and Misratah and Al Jabal al Gharbi in Libya.

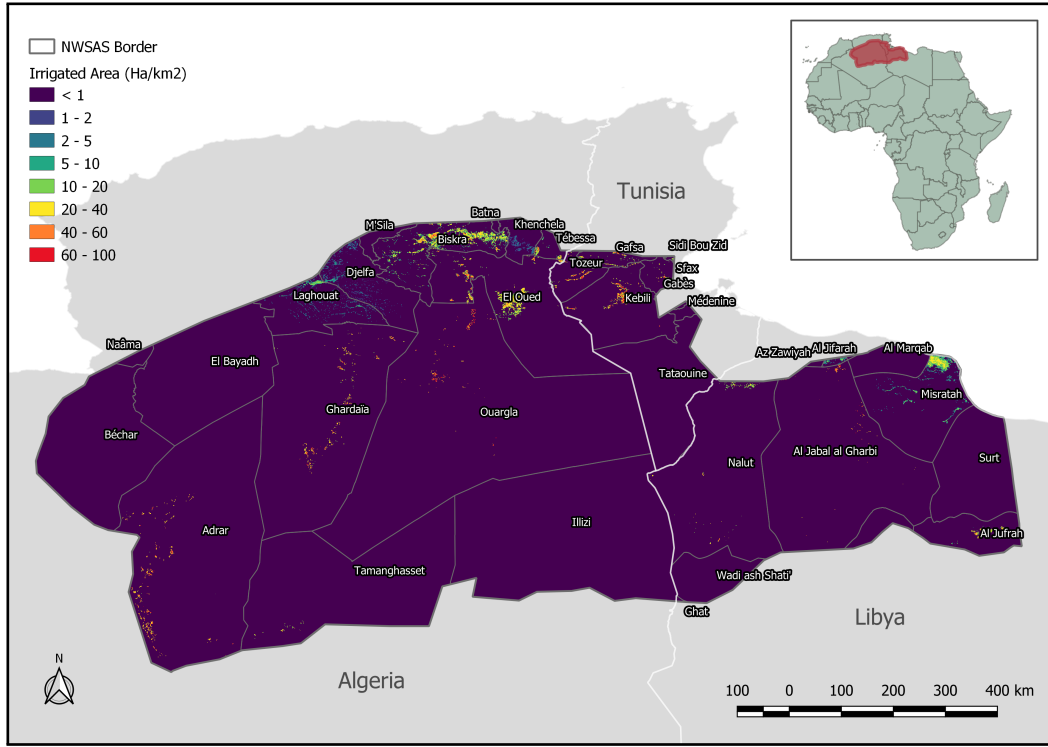


Figure 2. North Western Sahara Aquifer System - Cropland density map at 1×1 km grid cell resolution.

1.2. Population dataset

Individual population datasets for Algeria, Tunisia and Libya were obtained from the WorldPop database [10] in a resolution of 100×100 meters. Afterwards, the three datasets were merged together and masked within the boundaries of the aquifer. The data was then rescaled to a 1 km grid cell resolution and calibrated for year 2015 according to regional statistics (refer to Table 2).

Figure 3 depicts the obtained population layer for the NWSAS region. It is clear that the population agglomerations follow the same location pattern as the cropland areas: scattered through the region with higher concentrations at north of the aquifer. Within Algeria, the provinces with major population count are: Biskra, El Oued, Ouargla, Laghouat, Ghardaïa, Adrar and Djelfa. As for Tunisia, Kebili, Tozeur and Gafsa present the higher population counts, although much lower than the Algerian provinces previously mentioned. Moreover, the provinces with higher population count within Libya are Al Marqab, Misratah and Al Jabal al Gharbi.

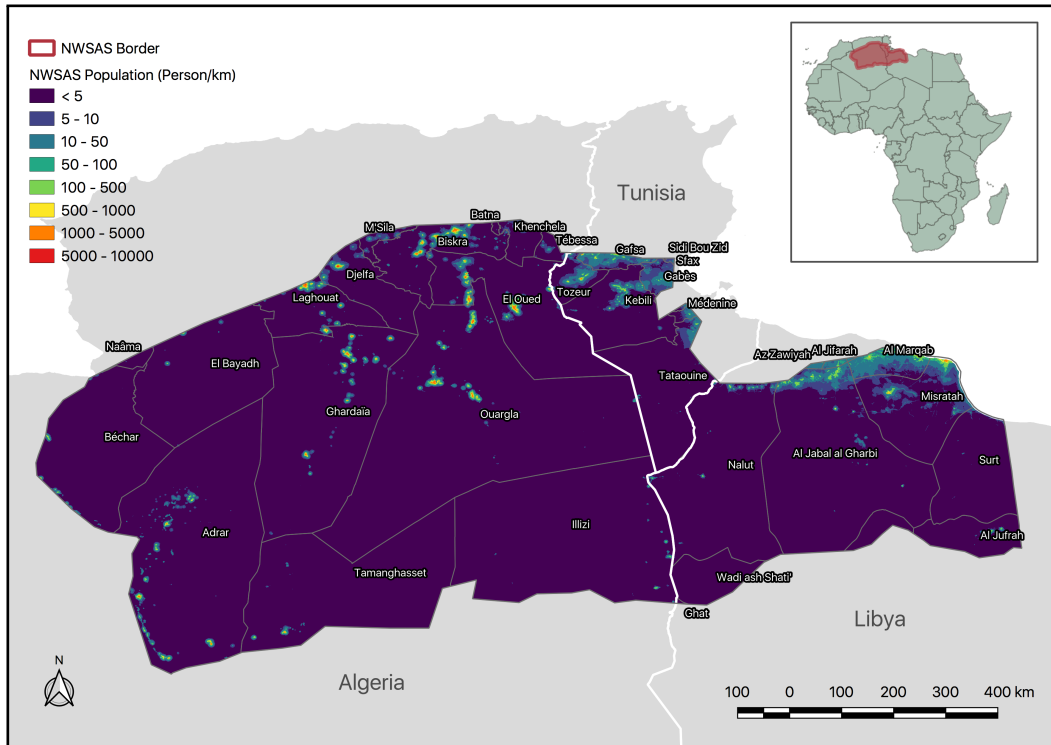


Figure 3. North Western Sahara Aquifer System - Population density map at 1×1 km grid cell resolution.

1.3. Depth to groundwater dataset

The depth to groundwater dataset used, was developed by the British Geological Survey for the African continent at a resolution of 5km grid cell. This dataset is underpinned by dedicated case studies and systematic data and literature reviews [3]. The dataset was masked with the NWSAS boundaries and aligned to match the target 1km grid cell resolution (Figure 4).

According to this data, it can be seen that the depth to groundwater through the entire aquifer ranges from around 50 to more than 250 meters. In general, in the south of the aquifer the deepest water tables can be found, which could mainly affect the population and agricultural activity of the province of Adrar and part of the provinces of Ouargla and Ghardaïa. To the north of the basin, the water table levels decrease to a range between 50 to 100 meters, which can be argued, enables the high agricultural activity there, specially in the province of Biskra.

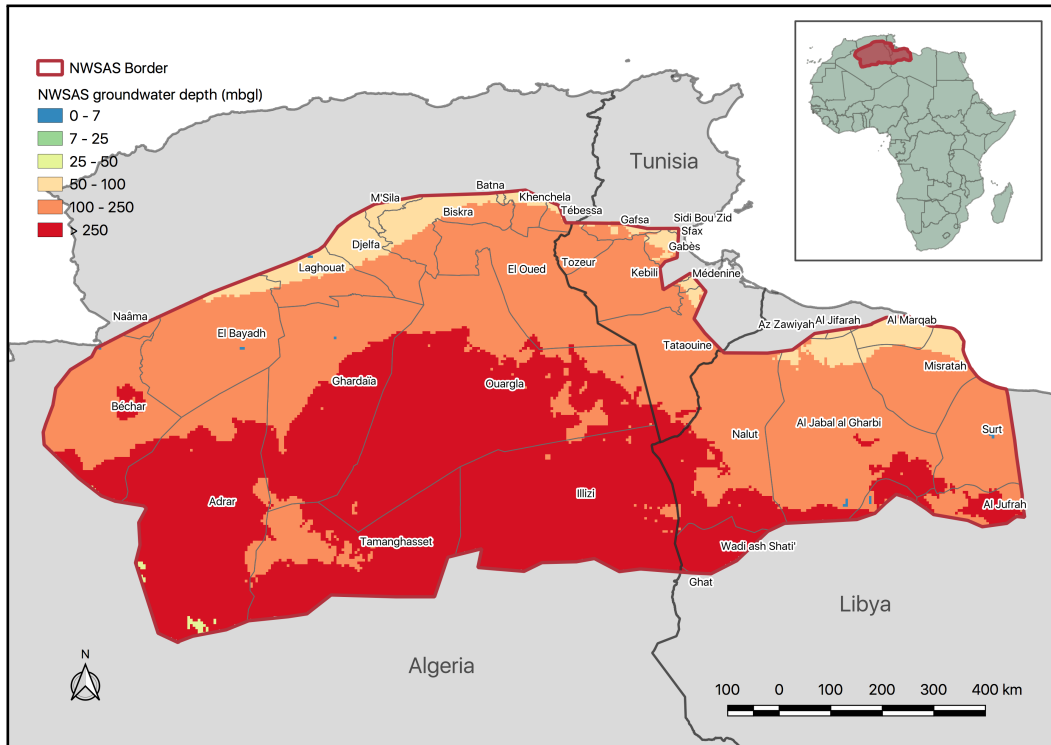


Figure 4. North Western Sahara Aquifer System - Depth to groundwater map at 1×1 km grid cell resolution.

2. Data calibration

The *population* and the *irrigated area* layers were calibrated to match regional statistics. The calibration was performed using the fraction given between the regional statistical data (i.e. total population or total irrigated area), and the sum of all data points of the layer in question. The statistical data was available as per country or provincial basis. Thus, the calibration process was performed for the basin areas within each country/province, using their specific information (see table 2 and table 3).

Table 2. NWSAS population and irrigated area statistics for year 2015, subdivided per country area inside the basin. Data source: [2, 8, 11]

Parameter	Total	Algeria	Tunisia	Libya
NWSAS Population	4,800,00	2,123,256	726,248	1,535,496
NWSAS Irrigated area (Ha)	281,194	202,275	40,371	38,548

Provincial data on irrigated land was derived from [12, 2, 8, 11]. Intensification rates for irrigated area were taken from [8] and used to account for a growth in irrigated land to year 2050. The intensification rate measures the current average rate of irrigated area over the feasible area to be irrigated in each region. Moreover, irrigation water use per hectare values were also taken from [8], and used as basis to characterize the Baseline scenario (table 3).

Table 3. Provincial input data for irrigated area and irrigation water use. Based on [12, 2, 8, 11]

Country	Province	Irrigated area (Ha)	Intensification rate (-)	Future irrigated area (Ha)	Water used (m ³ /Ha)
Algeria	Adrar	28,228	0.84	33,605	14,518
	Batna	-	0.84	-	13,520
	Biskra	60,000	0.80	75,000	12,383
	Bchar	-	0.84	-	13,520
	Djelfa	3,000	0.84	3,571	13,520
	El Bayadh	-	0.84	-	13,520
	El Oued	50,000	0.80	62,500	13,023
	Ghardaïa	20,441	0.84	24,335	13,520
	Illizi	-	0.84	-	13,520
	Khenchela	1,000	0.84	1,190	13,520
	Laghouat	5,000	0.84	5,952	13,520
	M'Sila	-	0.84	-	13,520
	Nama	-	0.84	-	13,520
	Ouargla	29,488	0.88	33,509	14,218
	Tamanghasset	1,118	0.84	1,331	13,520
	Tébessa	4,000	0.84	4,762	13,520
Libya	Al Jabal al Gharbi	7,635	0.80	9,544	9,134
	Al Jifarah	1,000	0.80	1,250	10,193
	Al Jufrah	6,925	0.80	8,656	9,134
	Al Marqab	-	0.98	-	10,001
	Az Zawiyah	-	0.80	-	10,193
	Misratah	18,333	0.80	22,916	9,134
	Nalut	4,655	0.80	5,819	9,134
	Surt	-	0.80	-	9,134
	Tripoli	-	0.80	-	10,193
	Wadi ash Shati'	-	0.80	-	9,134
Tunisia	Gabs	2,380	0.89	2,674	7,038
	Gafsa	5,441	0.90	6,046	13,266
	Kebili	23,837	0.98	24,323	16,813
	Mdenine	-	0.77	-	3,633
	Sfax	350	0.90	389	13,266
	Tataouine	-	0.77	-	3,633
	Tozeur	8,363	0.98	8,534	16,813

3. Domestic and irrigation water withdrawals

The calculation of total water withdrawals $ww_{tot,i}$ was performed according to Equation (1). Domestic water withdrawals were calculated as the product between the population count in each data cell (Pop_i) and the specific water demand per capita (wpc_i) for the region. Similarly, withdrawals from irrigated agriculture were calculated as the product between the irrigated area inside each data cell ($IrrArea_i$) and the specific water demand per cultivated hectare ($wpha_i$) for the region.

$$ww_{tot,i} = Pop_i \cdot wpc_i + IrrArea_i \cdot wpha_i \quad (1)$$

For the Baseline, a level of water withdrawals per capita wpc of 55 cubic meters per year was assumed with a population growth of 0.5% per year [13]. Moreover, all cropland area resultant from the calibration process was considered to be irrigated by groundwater resources in accordance with data from [12] (see table 4) and the water requirements per cultivated hectare $wpha$ to be according to table 3. Moreover, these values are changed depending on the irrigation water regime of each scenario. Finally, a growth in irrigated area was considered based on the intensification rate reported for each province (table 3).

Table 4. Irrigated and rain-fed cropland area in the NWSAS, year 2012. Data source: [12]

Water and land use	Whole aquifer	Algeria	Tunisia	Libya
Irrigated agricultural land (Ha)	270,000	202,000	30,000	38,000
Rain-fed agricultural land (Ha)			102,000	133,300

4. Groundwater pumping

The energy needs to pump water from groundwater resources is given by the required lift ($H - h$), the pressure drop due to fluid friction in the piping, and the pressure losses in valves and fittings. Pressure losses due to friction in the piping were found to be rather small compared to the lift requirements. Therefore, and due to lack of specific data on wells and boreholes in the region, the pressure losses due to friction in the piping and in valves and fittings were disregarded. The energy requirements (in watt-h) can then be estimated as (2) [14]:

$$E = \frac{Q \cdot (\rho \cdot g \cdot (H - h))}{\eta} \quad (2)$$

Where Q stands for the water extractions (m^3), ρ for the water density (kg/m^3), g for the gravitational acceleration (m/s^2), H for the delivered hydraulic head (meters), and h for the head in the well (meters). Moreover, η accounts for the pumping efficiency, which was set as 85% along the entire aquifer.

5. Energy-for-wastewater

To calculate the energy-for-wastewater requirements an energy intensity factor was used for each evaluated treatment technology following (3).

$$E_{ww} = Q_{ww,yr} \cdot X_t \quad (3)$$

Where $Q_{ww,yr}$ represents the yearly treated wastewater in m^3/yr , and X_t the average energy demand of the specific WWTT t , to treat one m^3 of wastewater (in kWh/m^3).

6. Wastewater Treatment System characteristics

FAO standards for population wastewater pollutant levels and reused water quality for agricultural irrigation [15], were used for the entire NWSAS area. These are shown in table 5.

Table 5. Pollutant levels of domestic wastewater and treated wastewater to be reused in agricultural irrigation. Based on [15].

Pollutant type	Domestic (mg/l)	Treated (mg/l)	Removal (%)
Suspended solids (SS)	700	30	95%
Nitrogen (N)	40	30	25%
Phosphorus (P)	20	10	50%
Biochemical Oxygen Demand (BOD_5)	500	50	90%
Chemical Oxygen Demand (COD)	1300	120	90%

Cost functions for different WWTT taken from the work of Molinos-Senante et al. [16], were used to evaluate the competence of selected technologies in the NWSAS. Energy intensity characteristics were added for each technology according to [17, 18]. The characteristics of the different WWTT and their cost and energy functions are presented in table 6.

Table 6. Treatment systems analyzed Adapted from [16], Copyright (2012), with permission from Elsevier.

Technology	Pollutant removal (%)	Costs (€)	Energy (kWh) [†]	Usage
Pond System (PS)	N: 20 – 40	CAPEX: $3897.7 \cdot x^{-0.407}$	$0.19 \cdot V$	Irrigation tailwater
	P: 60 – 70	OPEX: $5.543 \cdot x + 3127.5$		
	COD: 60 – 96			
	SS: 50 – 90			
Intermittent Sand Filter (ISF)	N: 65 – 95	CAPEX: $2115.5 \cdot x^{-0.399}$	$0.2 \cdot V$	Domestic wastewater
	P: 75 – 99	OPEX: $12.026 \cdot x + 3518.9$		
	COD: 75 – 90			
	SS: 85 – 95			

continued ...

... continued

Technology	Pollutant removal (%)	Costs (€)	Energy (kWh) [†]	Usage
Trickling Filter (TF)	N: 35 – 50 P: 35 – 55 COD: 75 – 90 SS: 50 – 90	CAPEX: $12237 \cdot x^{-0.87}$ OPEX: $13.504 \cdot x + 6020$	$0.3 \cdot V$	Domestic wastewater
Moving Bed Biofilm Reactor (MBBR)	N: 10 – 20 P: 30 – 40 COD: 20 – 40 SS: 60 – 80	CAPEX: $1187 \cdot x^{-0.165}$ OPEX: $12.794 \cdot x + 6031$	$0.8 \cdot V$	Domestic wastewater
Rotating Biological Contractors (RBC)	N: 20 – 80 P: 10 – 30 COD: 70 – 93 SS: 75 – 98	CAPEX: $6931.4 \cdot x^{-0.383}$ OPEX: $313.4 \cdot x^{-0.435}$	$0.8 \cdot V$	Domestic wastewater
Membrane Bioreactor (MBR)	N: 50 – 90 P: 20 – 70 COD: 70 – 90 SS: 85 – 99	CAPEX: $5635.3 \cdot x^{-0.352}$ *OPEX: $2.116 \cdot V^{0.713} e^{1.51 \cdot SS + 0.037 \cdot BOD}$	$0.8 \cdot V$	Domestic wastewater
Extended Aeration (EA)	N: 50 – 90 P: 15 – 70 COD: 70 – 90 SS: 85 – 99	CAPEX: $7946 \cdot x^{-0.460}$ *OPEX: $169.48 \cdot V^{0.454} e^{0.61 \cdot SS}$	$0.6 \cdot V$	Domestic wastewater
Sequencing Batch Reactor (SBR)	N: 55 – 90 P: 25 – 70 COD: 70 – 90 SS: 85 – 99	CAPEX: $8258.9 \cdot x^{-0.407}$ OPEX: $309.4 \cdot x^{-0.389}$	$1 \cdot V$	Domestic wastewater

x: population equivalent, $x = V \times 1500 / (400 \times 365)$, V: wastewater flow (m^3/yr)

N: Nitrogen, P: Phosphorus, COD: Chemical Oxygen Demand, SS: Suspended Solids

CAPEX: Capital Expenditure, OPEX: Operating Expenses

* Taken from [19]

† Based on [20, 18]

7. Reverse Osmosis desalination

Reverse Osmosis (RO) desalination is the most popular desalination technology used worldwide. Its energy intensity falls typically in the range of 0.5 to 2.5 kWh per cubic meter of desalinated brackish water [21, 22, 23].

To estimate the energy required to desalinate one cubic meter of saline water, often detailed information of the RO system is required. When analysing a broad area using a geospatial approach, such information is not available as the characteristics of the system can change from application to application [24, 25]. Thus, a simplified approach was used to estimate the RO energy requirements. RO is a pressure-driven process that forces water through a membrane which separates dissolved solutes using preferential diffusion. The output water from the membrane (*permeate*, p) is relatively free of solutes, while the remaining water (*concentrate*, c) exits the pressure vessel with

a high concentration of solutes (i.e. high TDS levels). A schematic representation of the process is presented in figure 5 [26].

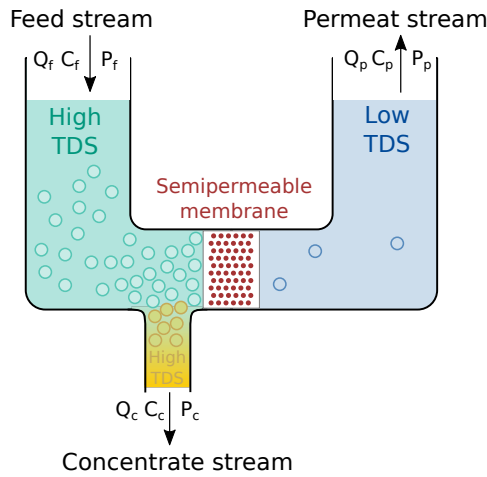


Figure 5. Reverse osmosis schematic separation process. Based on: [26].

The minimum energy required to push the water through the membrane is given by the amount of diluted solutes in the *feed* (*f*) water. Such minimum energy can be estimated calculating the osmotic pressure of the *feed* water, as described in (4) [26].

$$\pi = \phi \cdot C \cdot R \cdot T \quad (4)$$

Where:

- π : osmotic pressure (bar),
- ϕ : osmotic coefficient, close to 1 (-), assumed a 0.95 [26],
- C : concentration of all solutes (mol/L),
- R : universal gas constant, 0.083145 (L·bar/mol·K),
- T : absolute temperature (K), $(273 + {}^\circ\text{C})$, assumed at $25 {}^\circ\text{C}$ for the entire aquifer.

Thus, the minimum energy demand can be estimated multiplying the osmotic pressure of the *feed* water π (in bar) by a conversion factor of $1.0 \text{ kWh/m}^3 = 36 \text{ bar}$ and the *feed* brakish volum per year Q_y .

$$SEC_{min} = 36 \cdot \pi \cdot Q_y \quad (5)$$

In reality, the energy demanded is greater due to factors as friction losses, membrane filtration resistance, among others [22, 23]. Thus, values were taken from [22] to account for the additional energy needs.

Moreover, brine post treatment is key to prevent environmental impacts, such as water and soil salinization [23]. However, brine treatment and disposal can be an expensive process, therefore proper processes need to be design accounting for the region characteristics [23].

Table 7. Energy requirements for brackish water RO desalination. Adapted from [22], Copyright (2018), with permission from Elsevier.

Itemized SEC (kWh/m ³)	Brackish water
SEC_f membrane filtration resistance	0.194
SEC_R friction losses, retentate	0.036
SEC_P friction losses, permeate	0.0016
SEC_{CP} concentration polarization	0.005
SEC_{inef} pump & ERD inefficiency	0.068

ERD: energy recovery device

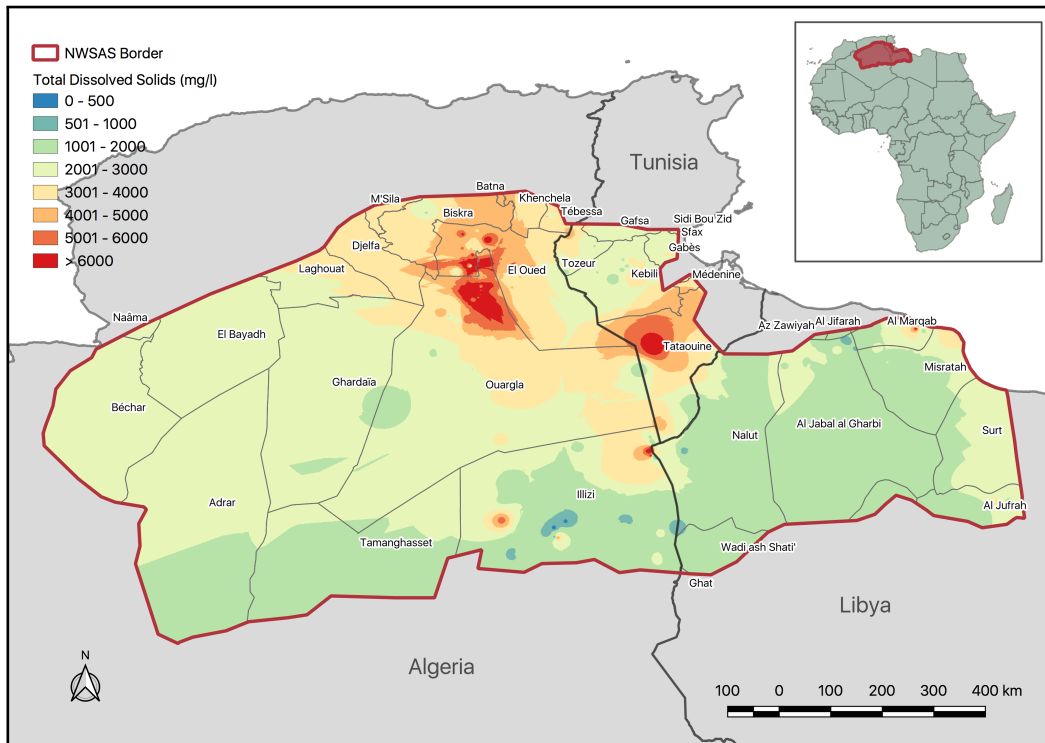


Figure 6. North Western Sahara Aquifer System - Groundwater quality map, Total Dissolved Solids (TDS) at 1×1 km grid cell resolution.

The water quality layer used, was obtained from 206 measurements provided by National Authorities of the region. Each point specifies the spacial location and groundwater TDS content. Although the data did not cover the entire basin area, due to lack of any other related information it was used to produced a raster layer. An inverse distance weighted interpolation method, having as distance weighting factor an inverse distance to a power of 2 and a global search radius with maximum number of nearest points of 10 was used (see figure 6).

8. Levelised Cost of Water (LCOW)

In this section the LCOW methodology is expanded as it could be beneficial for future work on the subject. This could aid on understanding what would be the efforts required as tax deductions, subsidies or reduced interest loans, for treated wastewater/tailwater to be competitive with local costs of water (what the farmer actually pays). The goal in the manuscript was to provide an overall picture, thus efforts could be concentrated in regions with high potential.

Equation 6, disaggregates the *LCOW* (\$/m³) value in three components: the cost components due to investment $LCOW_{Inv}$, operation and maintenance $LCOW_{O\&M}$ and externalities $LCOW_{Ext}$.

$$LCOW = LCOW_{Inv} + LCOW_{O\&M} + LCOW_{Ext} \quad (6)$$

All investment components used, need to be comprised in the CAPEX function of each WWTT. This enables the use of the values calculated with the CAPEX functions of each WWTT for each region or cluster, to easily calculate the $LCOW_{Inv}$ values for each specific technology and region/cluster. Equation 7 describes the process to calculate the $LCOW_{Inv}$.

$$LCOW_{Inv} = \frac{Inv}{\sum_{t=1}^T V_t \cdot \gamma^t} \cdot \Delta \quad (7)$$

Where Inv stands for the CAPEX value, V_t for the treated water flow per year t (m³/yr), Δ for the tax factor (Equation 9) and γ^t represents the discount factor of the project (Equation 8).

The discount factor is an important term, as the LCOW methodology represents a break-even investment for the stakeholders, thus an appropriate discount rate (r) needs to be used to ensure the right amount of return needed for all sources of long term capital (i.e. equity holders and debt). Often, the proper discount rate used is the WACC [27]. The discount factor is then calculated according to the discount rate r , as shown in (8). A discount rate of $r = 5\%$ was used for this study, with a sensitivity analysis on lower (3%) and higher (8%) values.

$$\gamma^t = \left(\frac{1}{1+r} \right)^t \quad (8)$$

The tax factor Δ includes all effects of the tax related variables, however, region specific tax data was not available either collect or derive, thus the tax factor was set equal to 1. Nonetheless, such parameter could be useful to analyse policies taking incentives in tax deductions which could aid the adoption of treated wastewater reuse. The tax related variables are the rent tax α , depreciation d_t , depreciation period T , discount factor γ and investment tax credit i . Equation 9 describes the way of obtaining the tax factor.

$$\Delta = \frac{1 - i - \alpha \cdot \sum_{t=1}^T d_t \cdot \gamma^t}{1 - \alpha} \quad (9)$$

Moreover, the LCOW related to operational costs $LCOW_{O\&m}$ (Equation 10) can be computed by using the OPEX values ω_t calculated for each year, in each region/cluster — using the cost-functions of each WWTT evaluated— and the discount factor γ^t per year.

$$LCOW_{O\&m} = \frac{\sum_{t=1}^T \omega_t \cdot \gamma^t}{\sum_{t=1}^T V_t \cdot \gamma^t} \quad (10)$$

Furthermore, the avoidance of externalities due to the discharge of untreated wastewater to the environment can also be included in the LCOW value, which may help to render a WWTP economically viable. This parameter was not included in the current analysis due to lack of data, however it is expanded here as it can be valuable for future work on other regions or detailed analysis in the NWSAS region. The logic behind this idea, falls in the fact that by treating and reusing wastewater, the pollutants presented in the contaminated water streams are prevented to run into fresh water bodies, rivers or groundwater aquifers. Thus, by defining a monetary value to the prevention of pollutants going into ecosystems, the economic environmental benefits can be internalised [16]. The externalities-related LCOW value $LCOW_{Ext}$ (Equation 11) can be obtained as follows:

$$LCOW_{Ext} = \frac{\sum_p^P \sum_{t=1}^T m_p \cdot B_p \cdot V_t \cdot \gamma^t}{\sum_{t=1}^T V_t \cdot \gamma^t} \quad (11)$$

Where m_p represents the concentration of pollutant of class p avoided with the treatment of one cubic meter of wastewater (kg/m^3), and B_p the environmental benefit of avoiding one kilogram of pollutant p running into the environment ($\$/\text{kg}$).

9. Clusters

The 40 population and cropland clusters identified are presentd in Figure 7.

Clusters are numbered from 0 to 39, yielding 40 agglomerations including each population and cropland areas. Every cluster is tagged with a number and colored to make them stand out from others.

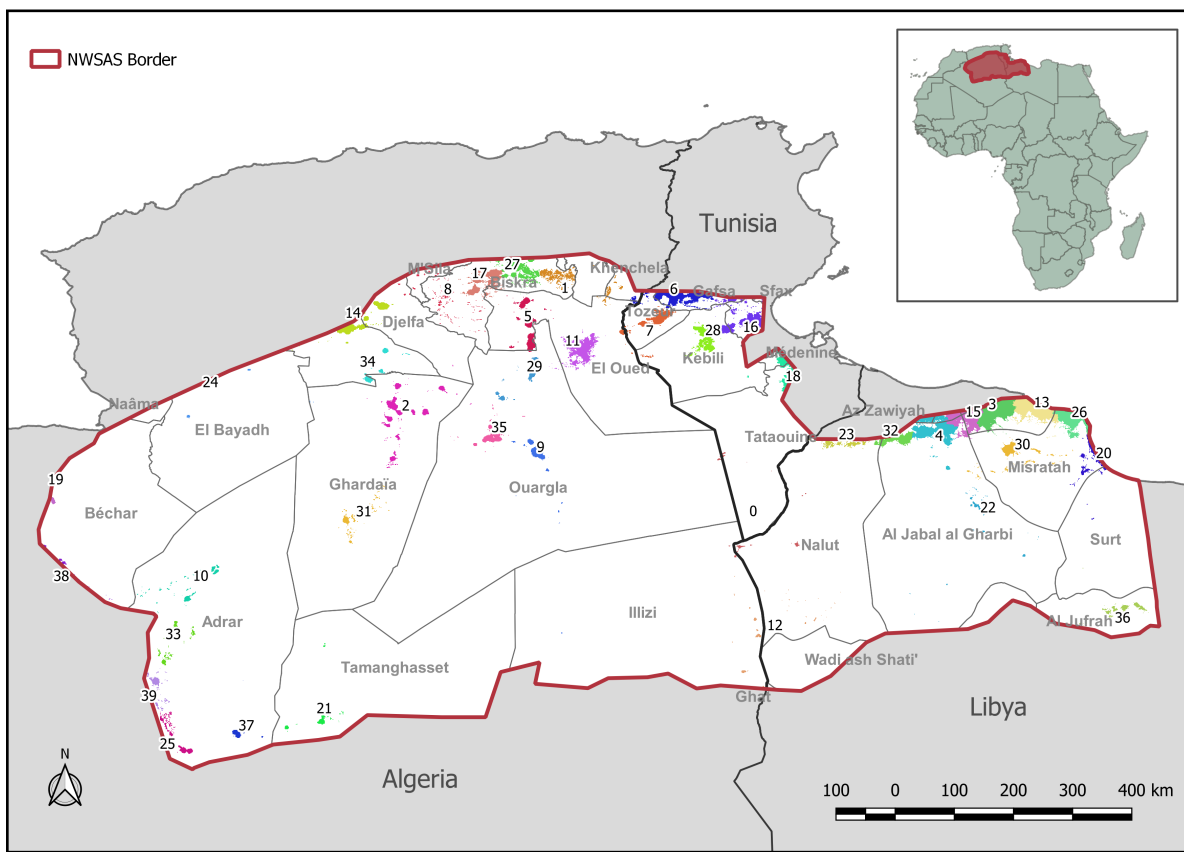


Figure 7. Population and cropland clusters. Clusters are numbered from 0 to 39, yielding 40 agglomerations including each population and cropland areas. Every cluster is tagged with a number and colored to make them stand out from others. The grey administrative boundaries correspond to the different provinces.

10. Water withdrawals and reuse per cluster

Additional results on water withdrawals and reuse per cluster, are reported in this section. Table 8, shows an overview of the total withdrawals per scenario, whereas figures 8 to 12 present detailed per cluster results.

Table 8. Summary of water results by scenario. Values calculated for the entire aquifer (total), as well as the minimum (min), maximum (max), average (mean) and median values between the clusters.

Parameter	Value	Scenario				
		Baseline	Scenario 1	Scenario 2	Scenario 3	Scenario 4
Water withdrawals (MCM)	total	4141.7	2342.6	2244.6	2388.4	3958.1
	min	0.6	0.6	0.6	0.6	0.6
	max	502.6	284.2	284.2	284.9	494.3
	mean	103.5	58.6	56.1	59.7	99.0
	median	49.1	23.6	23.6	25.5	44.7
Water reused (MCM)	total	0	1669.3	1022.1	2264.0	2385.0
	min	0.0	0.0	0.0	0.0	0.0
	max	0	212.4	119.1	296.5	304.4
	mean	0	41.7	25.6	56.6	59.6
	median	0	15.7	13.2	28.1	29.3
Water savings (MCM)	total	0.0	1799.1	1897.2	1753.4	183.7
	min	0.0	0.0	0.0	0.0	-27.1
	max	0.0	218.5	225.0	217.7	66.7
	mean	0.0	45.0	47.4	43.8	4.6
	median	0.0	19.0	19.5	17.1	2.9

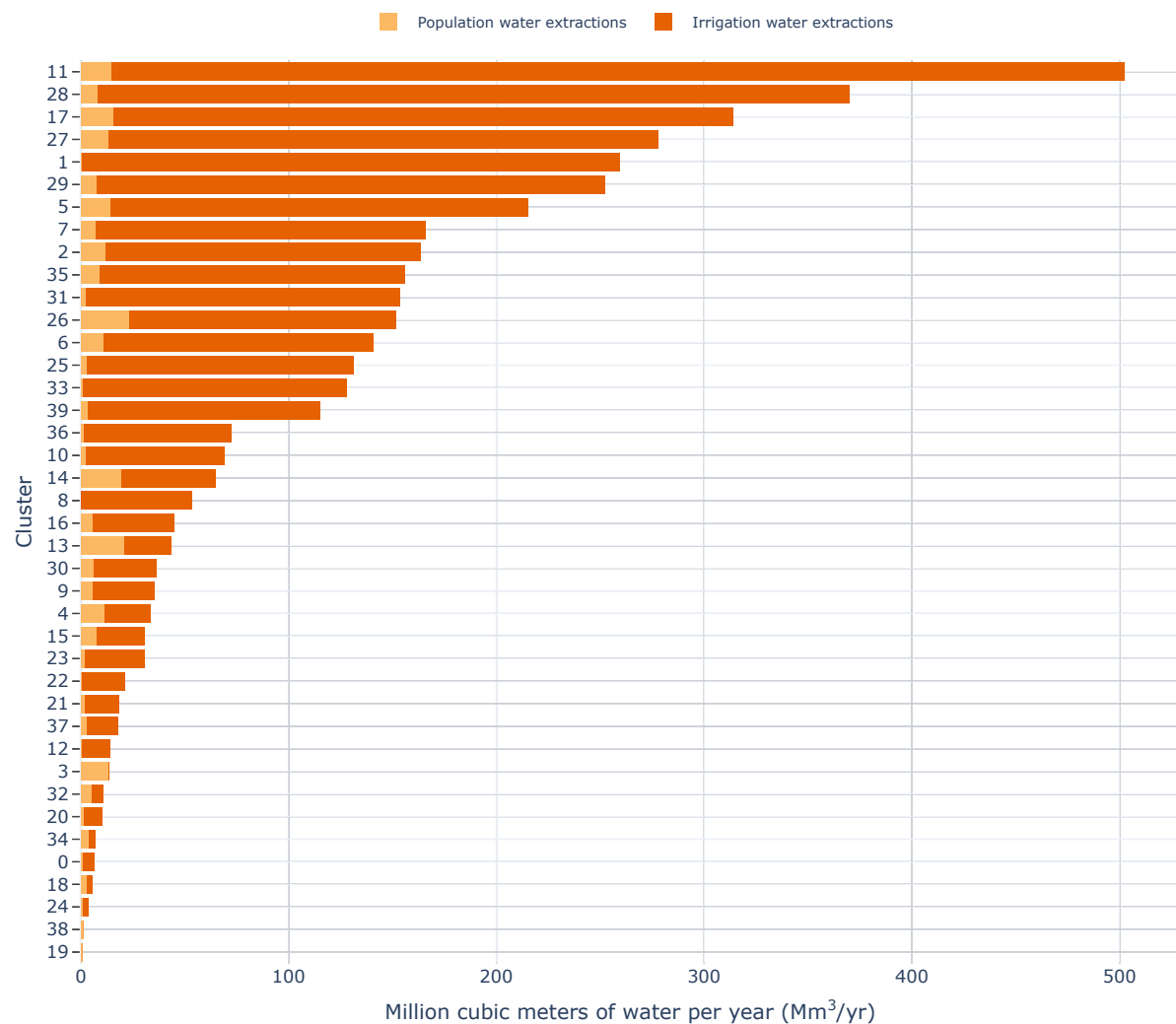


Figure 8. Water withdrawals by cluster. Baseline scenario.

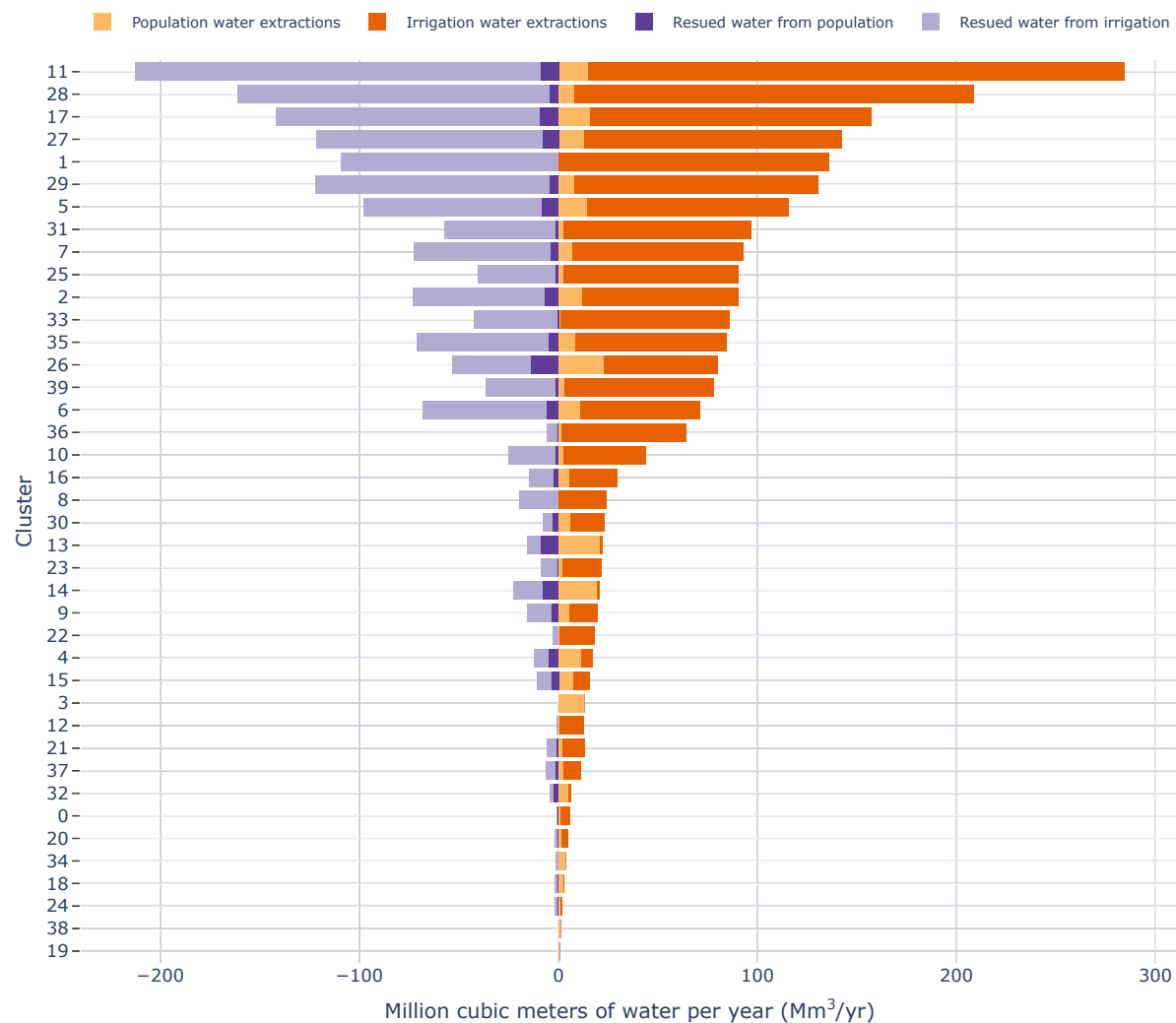
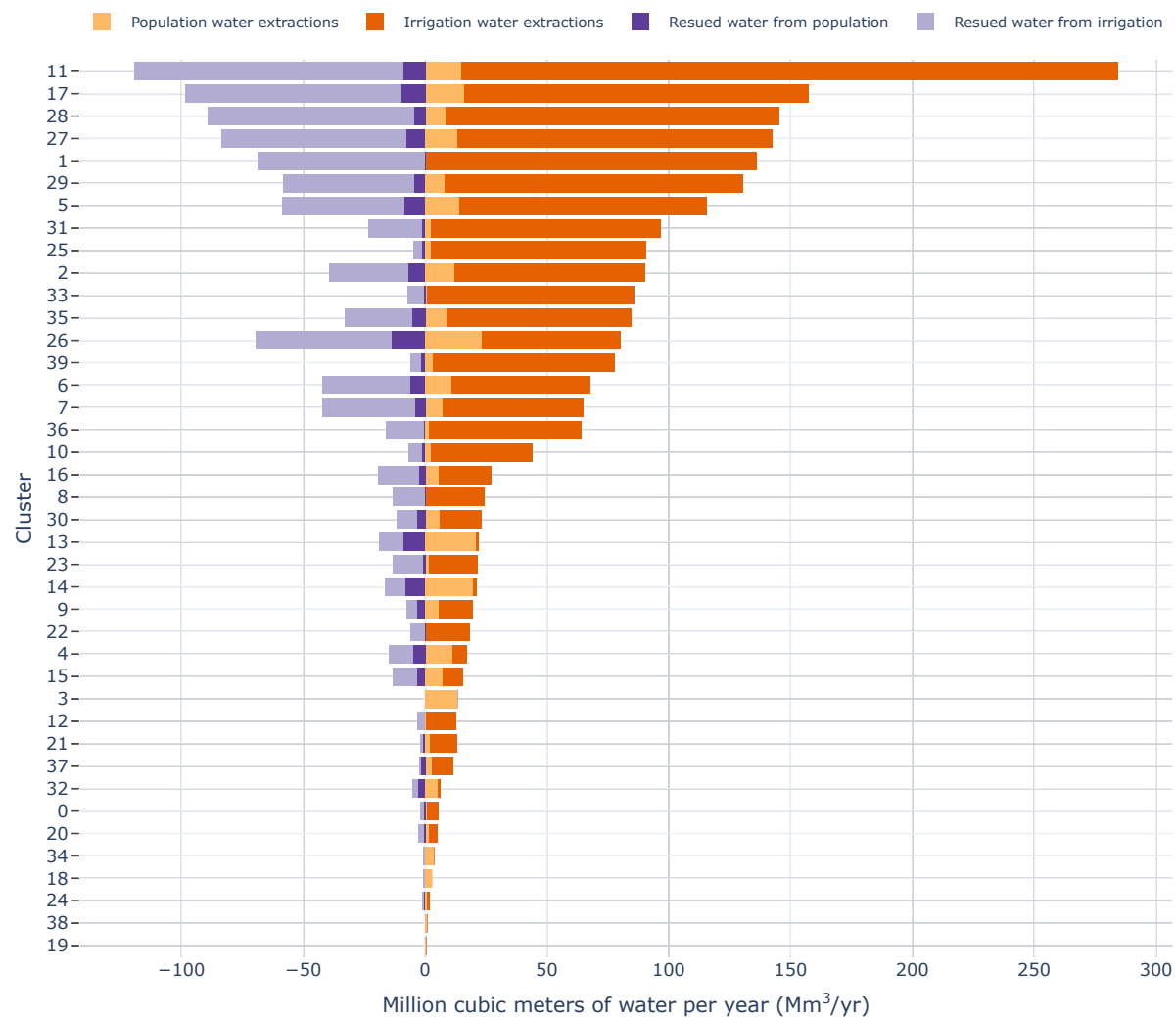


Figure 9. Water withdrawals and reuse by cluster. Scenario 1.

**Figure 10.** Water withdrawals and reuse by cluster. Scenario 2.

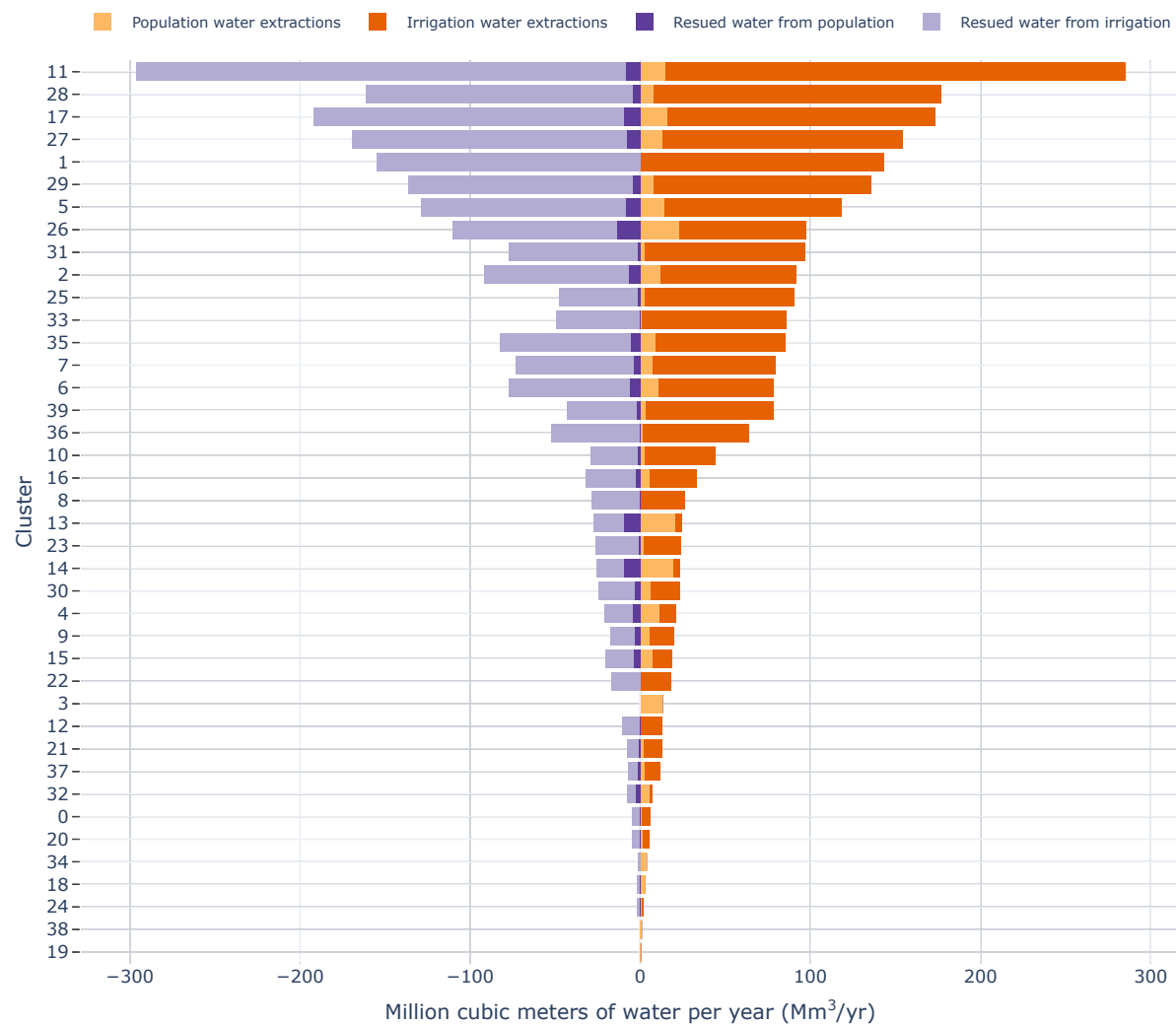


Figure 11. Water withdrawals and reuse by cluster. Scenario 3.

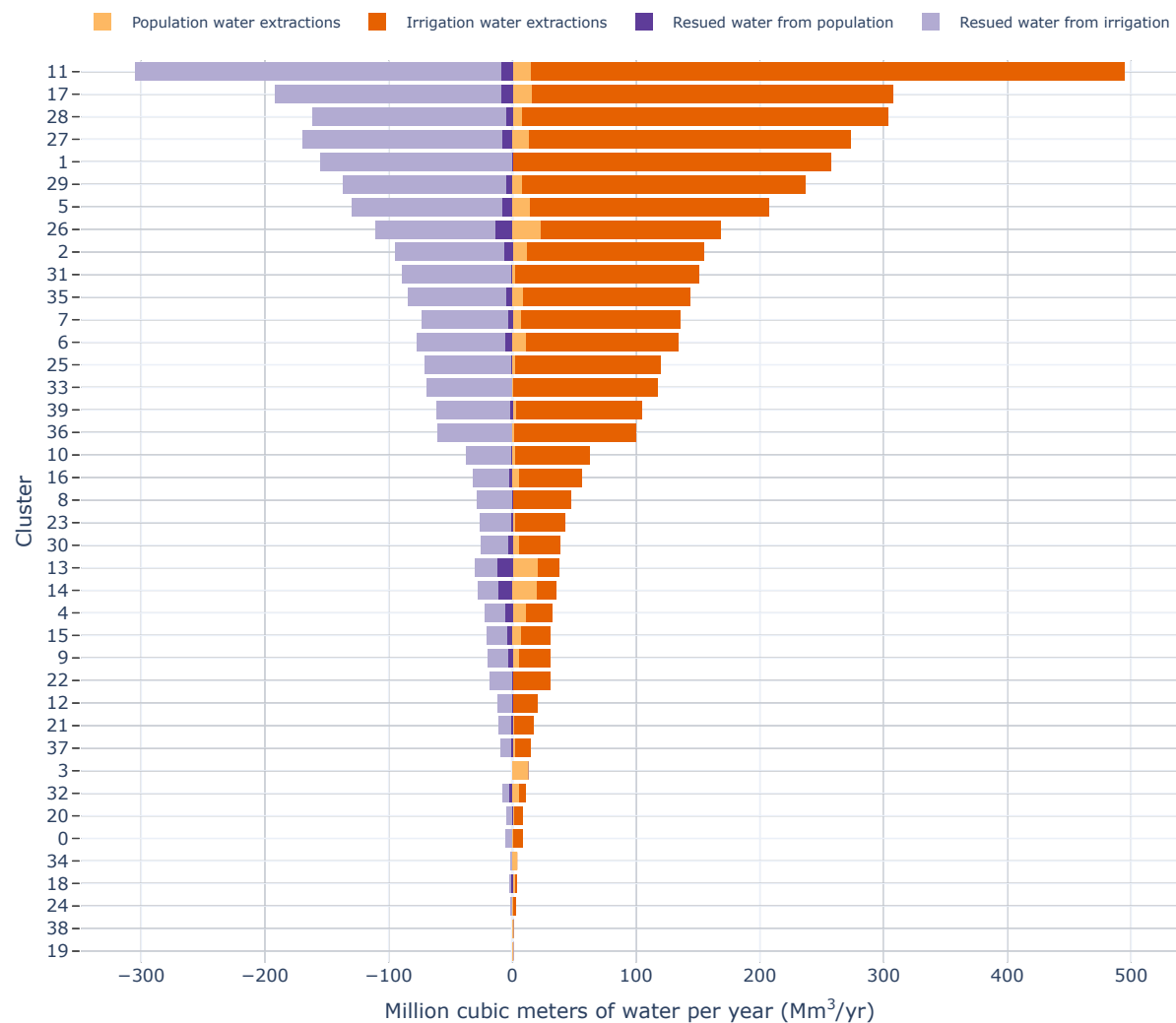


Figure 12. Water withdrawals and reuse by cluster. Scenario 4.

11. Energy demand per cluster

In this section, additional results concerning the energy requirements for water pumping, water desalination and wastewater treatment are presented. An overview for each scenario can be found in table 9, presenting total, min, max, mean, and median values. Moreover, figures 13 to 17 show detailed per cluster results.

Table 9. Summary of results by scenario. Selected results are calculated for the entire aquifer (total), as well as the minimum (min), maximum (max), average (mean) and median values between the clusters.

Parameter	Value	Scenario				
		Baseline	Scenario 1	Scenario 2	Scenario 3	Scenario 4
Energy (GWh)	total	3055.7	2153.3	2005.0	2223.6	3515.9
	min	0.5	0.6	0.6	0.6	0.6
	max	402.8	288.5	274.0	302.1	491.3
	mean	76.4	53.8	50.1	55.6	87.9
	median	26.7	19.9	19.8	21.6	34.1

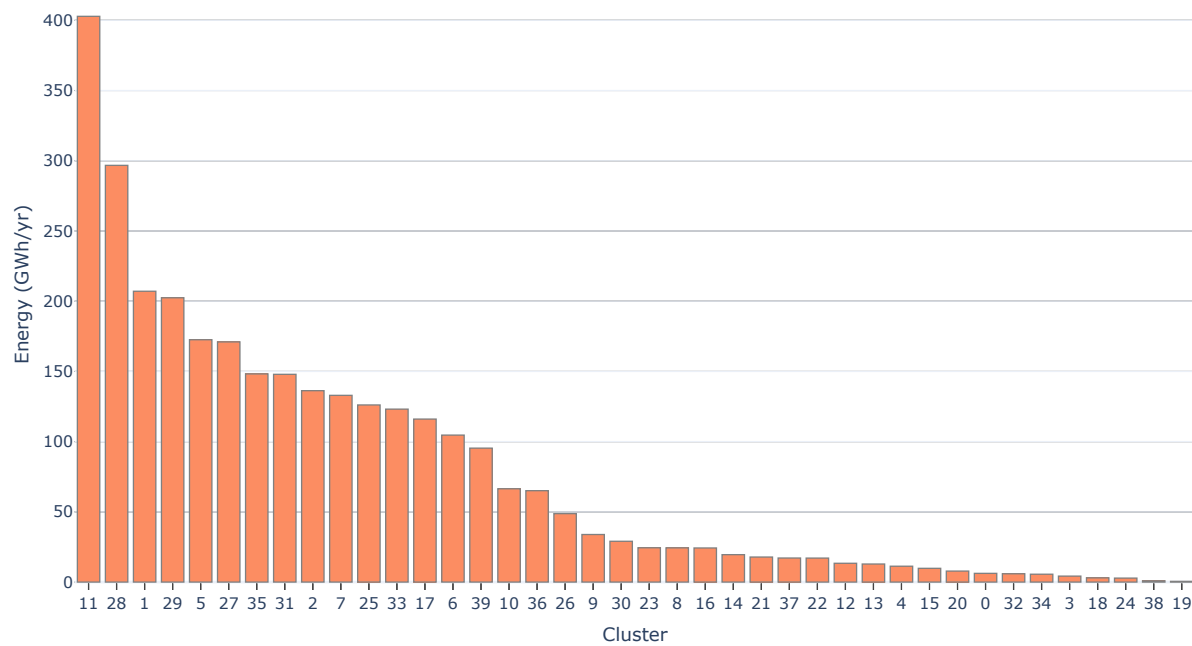
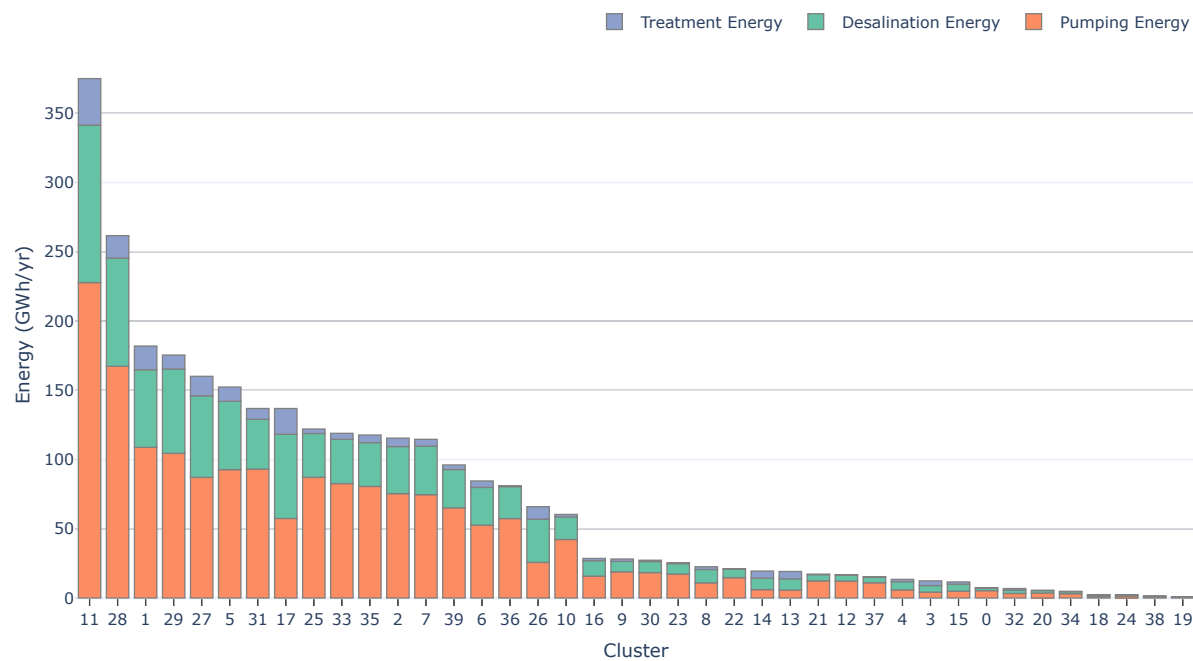
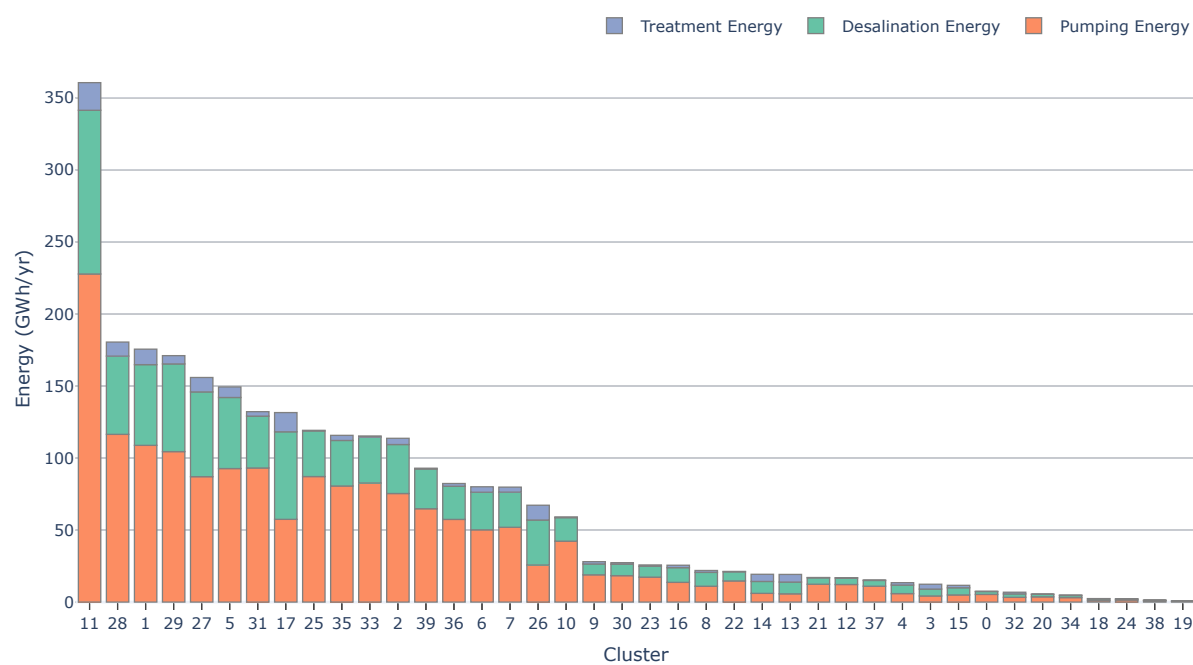
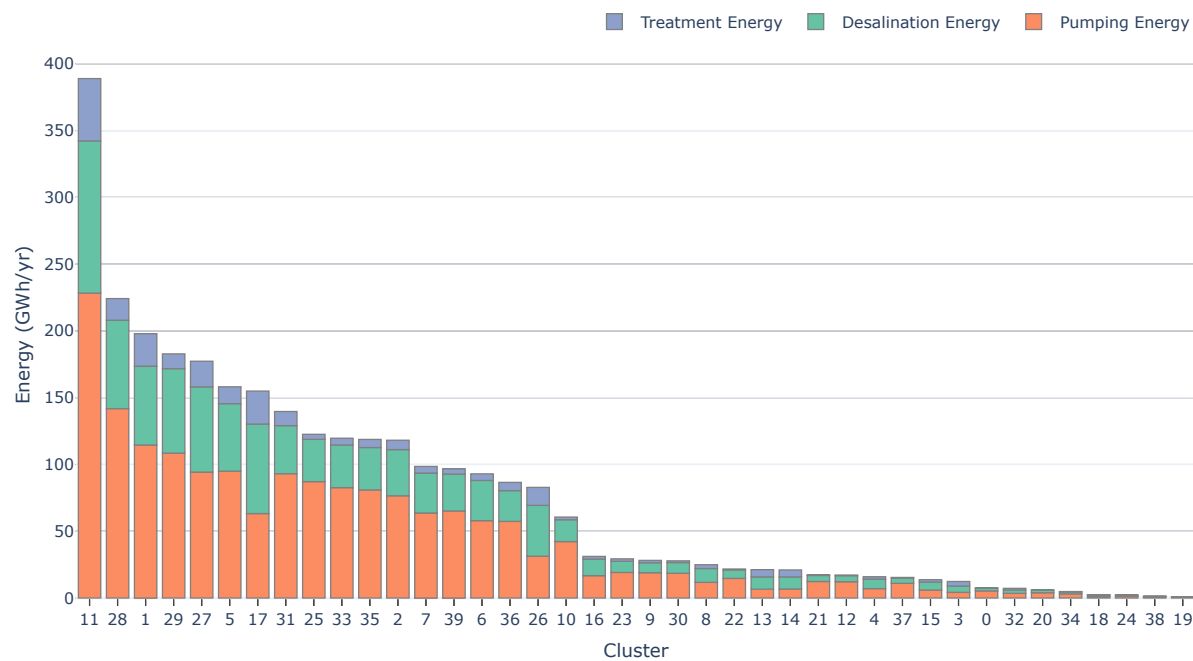
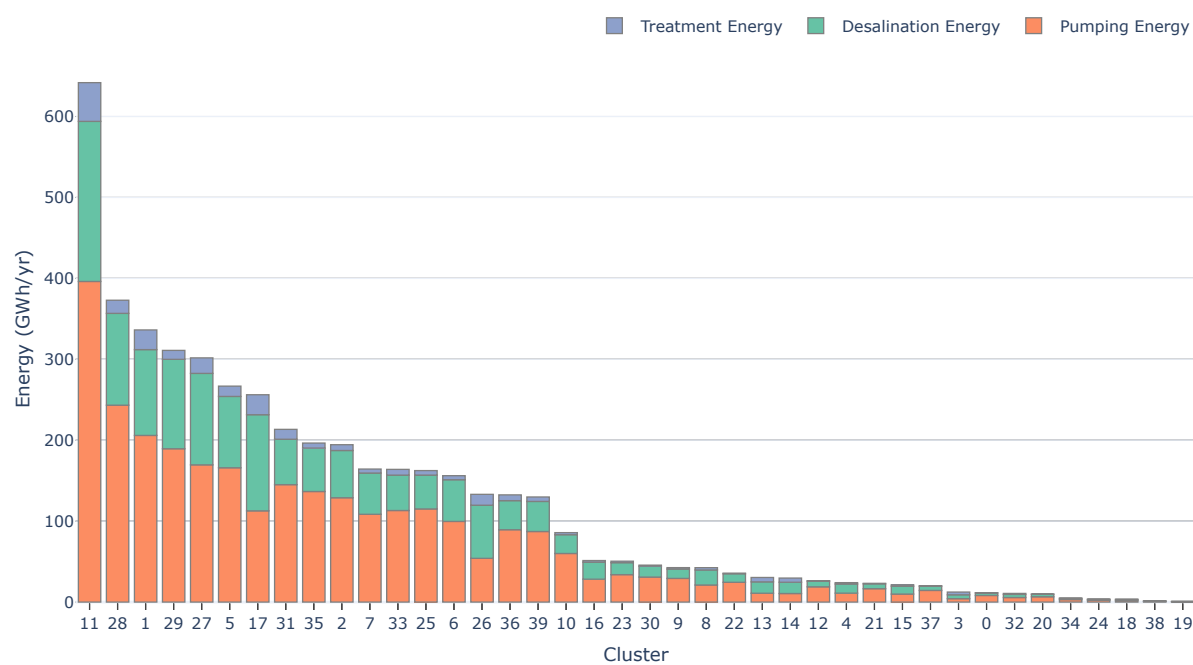


Figure 13. Energy requirements per cluster for pumping in the Baseline scenario.

**Figure 14.** Energy requirements per cluster for pumping in Scenario 1.**Figure 15.** Energy requirements per cluster for pumping in Scenario 2.

**Figure 16.** Energy requirements per cluster for pumping in Scenario 3.**Figure 17.** Energy requirements per cluster for pumping in Scenario 4.

12. Least-cost technologies

This section expands the results on least-cost technologies identified. The least cost options, are highly dependent on the treatment capacity needed, to show this more clearly, a subset of the largest clusters (in terms of water use) is done in figure 18. from there, it can be seen that the technologies LCOW values can vary largely if water withdrawals (or capacity) changes. Take for example cluster 1. It has very large irrigation water extractions, which makes the on-farm pond system to be cheap for tailwater treatment, however, the treatment technology options available for domestic wastewater all have fairly large values. This is due to the low water uses of the domestic sector in this cluster, which is driven by low population near the agricultural areas.

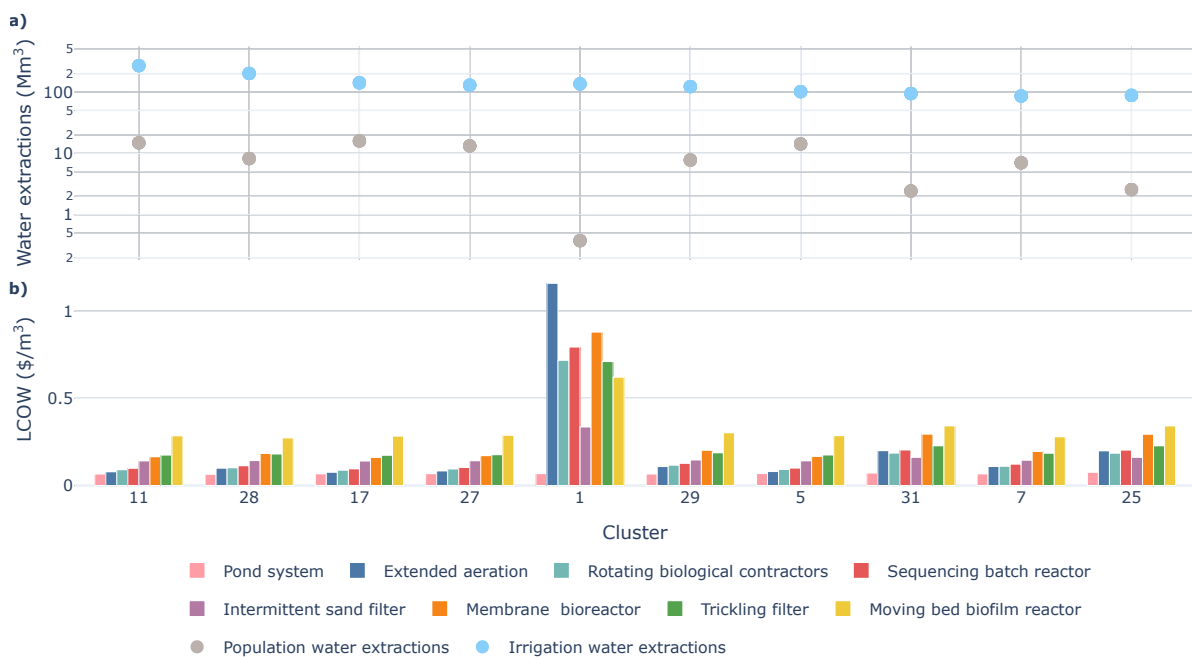


Figure 18. Energy requirements for pumping change due to groundwater depth increase. This was calculated for Scenario 1 and all pumping requirements throughout the basin were aggregated

Moreover, detailed maps of the technologies chosen for domestic wastewater treatment can be seen in figures 19, 20 and 21, for different domestic water uses. From figure 19, it can be seen that with lower water usage, the technology mix is richer throughout the basin, whereas when water use get higher (figure 20 and figure 21) all clusters then to prefer extended aeration. This is due to the economy of scale identified in figure 18, which shows a trade-off between the least-cost technology and the treatment capacity requirements.

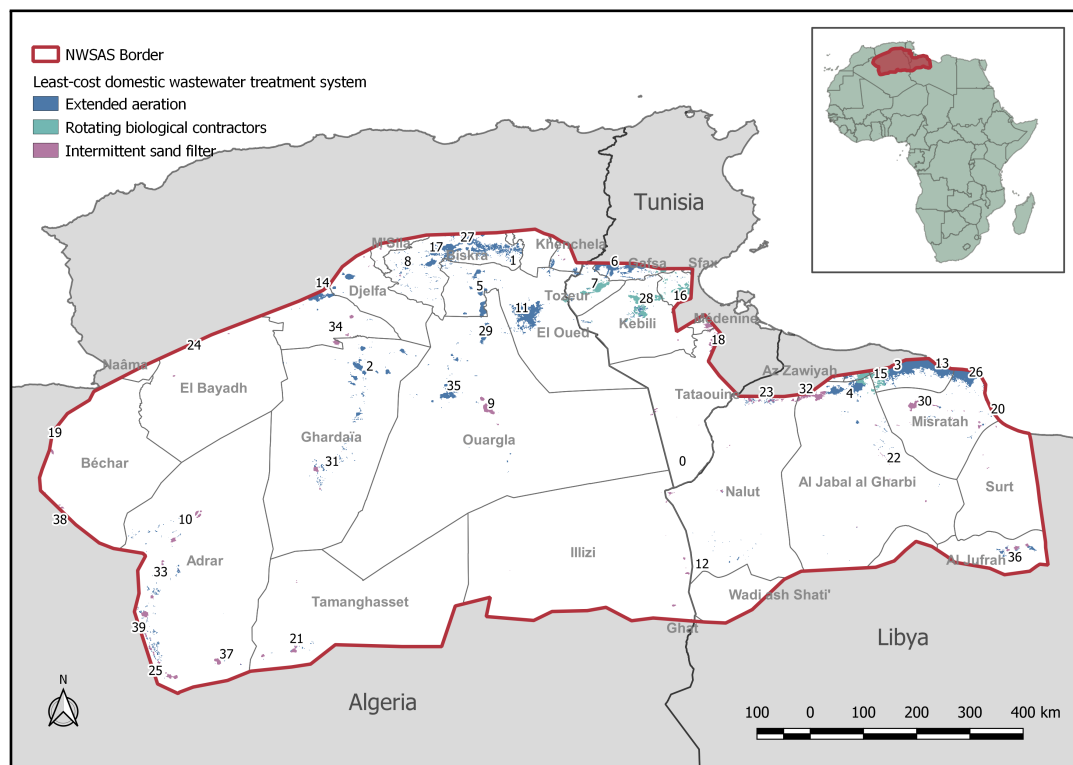


Figure 19. Least-cost domestic wastewater treatment system, with low domestic water use ($36 \text{ m}^3/\text{yr}$).

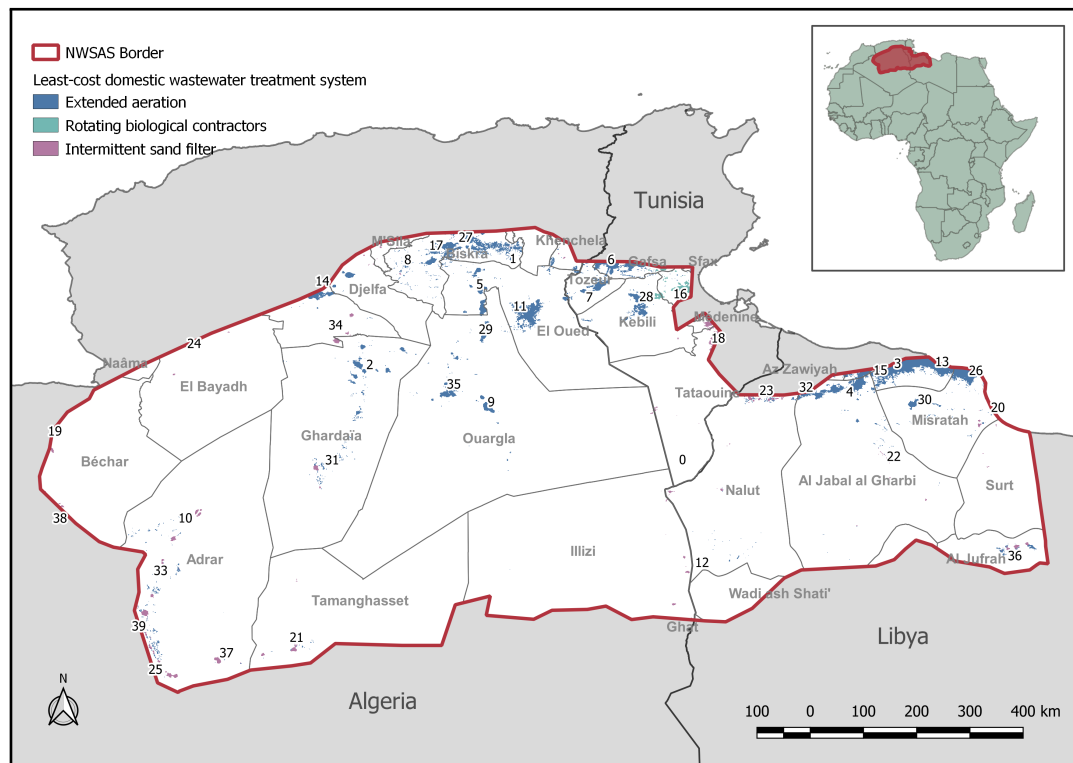


Figure 20. Least-cost domestic wastewater treatment system, with low domestic water use ($55 \text{ m}^3/\text{yr}$).

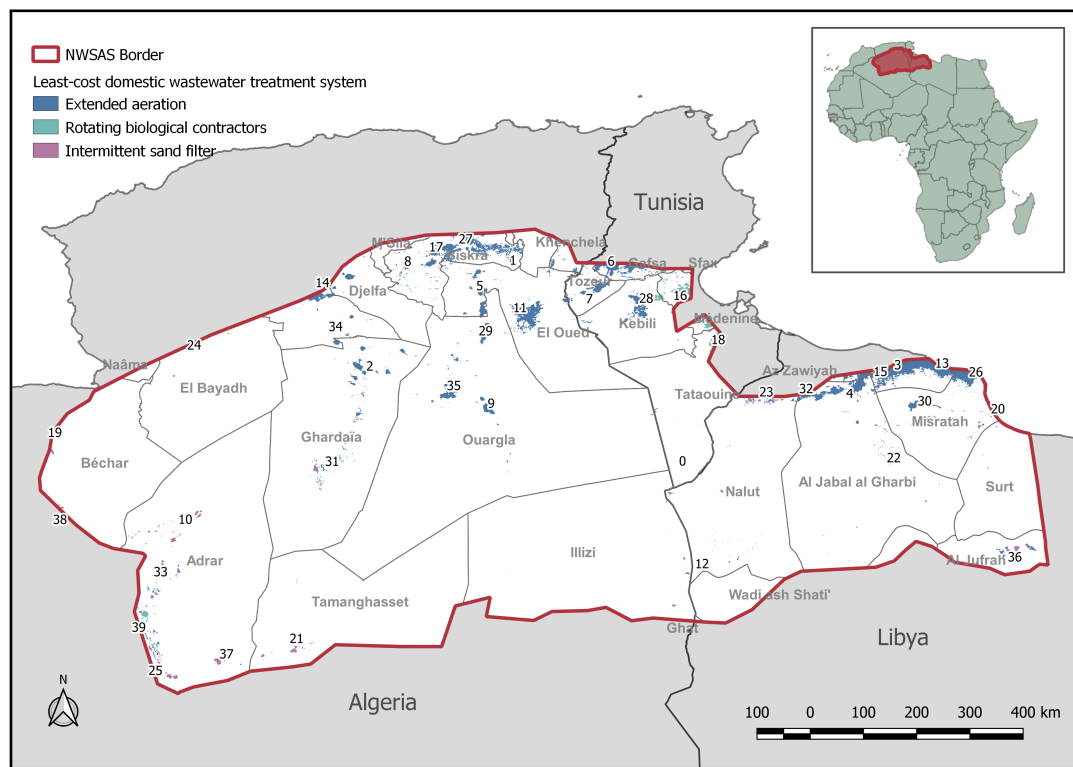


Figure 21. Least-cost domestic wastewater treatment system, with low domestic water use ($73 \text{ m}^3/\text{yr}$).

13. Sensitivity analysis

Sensitivity analysis were performed on key modeling parameters. This, helps to give clarity on uncertainties associated to the input data. All the sensitivity parameters evaluated are presented in table 10 and were calculated for Scenario 1 and an average year, unless stated differently.

Table 10. Selected sensitivity parameters with low, medium and high values. For the parameters that express a change (e.g. Depth to groundwater change), the change is measured against the current levels considered on the Baseline. All sensitivity parameters are evaluated for an average year of the evaluated period.

Parameter	Low	Medium	High
Domestic water per capita (m ³ /yr)	36	55	73
Population annual growth (%)	2	3	-
Depth to groundwater change (m)	0	+25	+50
Groundwater quality change (%)	-50	0	+50
Irrigated area increase (%)	10	20	40
Min TDS levels to desalinate (mg/l)	500	1000	2000
Discount rate (%)	3	5	8

13.1. Groundwater depth increase

Three levels of Groundwater depth increase were assessed: none, medium (25 meters change over a period of circa 17 years) and high (50 meters change over a period of circa 17 years). These values were selected as the current drawdown observed in the NWSAS is in average 1.41 meters per year [12]. Groundwater depth increase has a direct impact in energy requirements for pumping. These can be seen in figure 22 and figure 23. The overall increase in pumping energy requirements represent around 22% more energy in the high value case. This is a considerable amount of energy, which needs to be foreseen for long-term energy system planning.



Figure 22. Energy requirements for pumping change due to groundwater depth increase. This was calculated for Scenario 1 and all pumping requirements throughout the basin were aggregated

	Groundwater depth increase (meters)		
	none	medium: 25 meters	high: 50 meters
39.0 -	65.12	71.38	77.65
38.0 -	0.9	0.98	1.06
37.0 -	11.02	11.94	12.86
36.0 -	57.39	62.51	67.64
35.0 -	80.57	87.36	94.14
34.0 -	3.11	3.42	3.73
33.0 -	82.64	89.53	96.42
32.0 -	3.29	3.81	4.32
31.0 -	93.09	100.84	108.6
30.0 -	18.35	20.18	22.01
29.0 -	104.45	114.89	125.34
28.0 -	167.34	184.07	200.8
27.0 -	87.11	98.53	109.95
26.0 -	25.71	32.13	38.56
25.0 -	87.15	94.41	101.67
24.0 -	1.45	1.6	1.75
23.0 -	17.29	19.02	20.75
22.0 -	14.68	16.14	17.6
21.0 -	12.38	13.42	14.45
20.0 -	3.64	4.03	4.42
19.0 -	0.52	0.57	0.62
18.0 -	1.08	1.31	1.54
17.0 -	57.44	70.05	82.65
16.0 -	15.8	18.18	20.56
15.0 -	4.96	6.2	7.44
14.0 -	6.06	7.74	9.42
13.0 -	5.73	7.49	9.25
12.0 -	12.21	13.25	14.29
11.0 -	227.74	250.52	273.29
10.0 -	42.28	45.8	49.32
9.0 -	18.93	20.51	22.09
8.0 -	10.99	12.94	14.89
7.0 -	74.61	82.07	89.53
6.0 -	52.56	58.25	63.93
5.0 -	92.69	101.96	111.23
4.0 -	5.89	7.25	8.61
3.0 -	4.24	5.3	6.36
2.0 -	75.36	82.59	89.83
1.0 -	108.8	119.71	130.62
0.0 -	5.33	5.77	6.22

Figure 23. Energy requirements for pumping change due to groundwater depth increase. This was calculated for Scenario 1 for each cluster.

13.2. TDS content

The effect that TDS content of groundwater has on desalination energy requirements, was evaluated through 2 different ways: 1) three levels of low, medium and high TDS concentration, varying the concentration levels by -50%, 0% and +50% from current levels; and 2) by changing the TDS content threshold required to desalinate brackish water. The later values, were picked based on FAO recommendations for water quality for irrigation [15], where concentration below 450 mg/l have low or nonexistent impact, and concentrations from 450 to 2000 have slight to moderate impact. The outcomes of this analysis can be seen in figure 24 to 26. In general, the total content of TDS seems to have a higher effect on desalination energy demand.

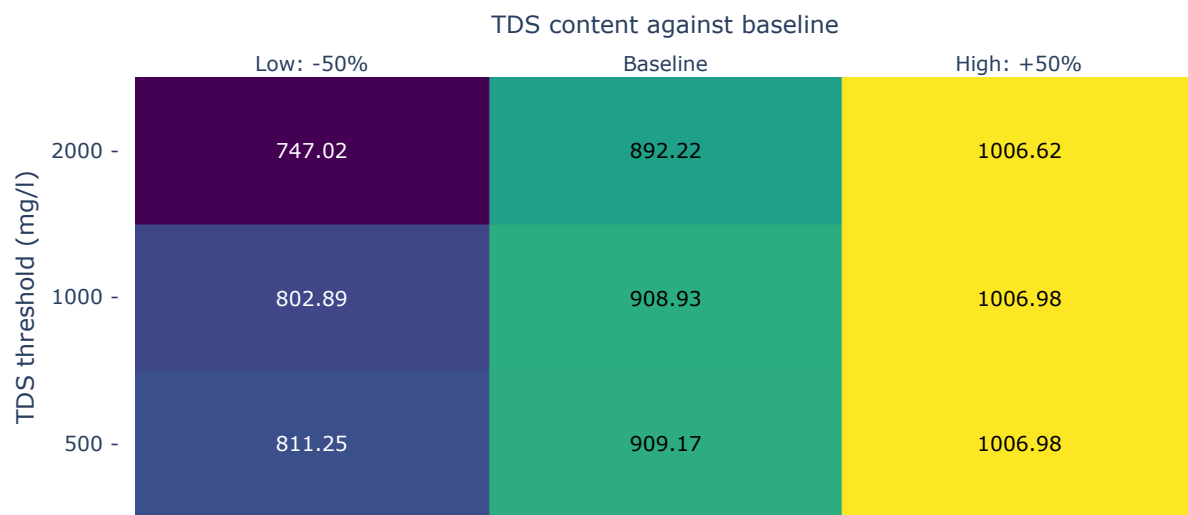


Figure 24. Energy requirements for desalination (GWh/yr) due to TDS content change in groundwater. This was calculated for Scenario 1 and all desalination energy requirements throughout the basin were aggregated

Cluster	TDS content against baseline		
	Low: -50%	Baseline	High: +50%
39.0 -	24.36	27.67	29.61
38.0 -	0.34	0.37	0.4
37.0 -	3.49	4.0	4.26
36.0 -	20.32	23.03	24.81
35.0 -	28.68	31.62	34.54
34.0 -	1.32	1.47	1.61
33.0 -	29.06	31.95	34.83
32.0 -	2.17	2.39	2.61
31.0 -	32.73	35.98	39.23
30.0 -	6.97	8.0	8.51
29.0 -	50.29	60.88	71.47
28.0 -	69.99	78.04	85.26
27.0 -	51.15	58.9	66.64
26.0 -	27.83	31.25	34.67
25.0 -	27.6	31.66	33.69
24.0 -	0.62	0.68	0.74
23.0 -	6.58	7.55	8.03
22.0 -	5.53	6.35	6.76
21.0 -	3.92	4.5	4.79
20.0 -	1.61	1.79	1.94
19.0 -	0.22	0.24	0.26
18.0 -	1.0	1.15	1.29
17.0 -	54.22	60.77	67.2
16.0 -	10.12	11.18	12.25
15.0 -	4.71	4.98	5.43
14.0 -	7.33	8.26	9.2
13.0 -	7.3	8.16	8.89
12.0 -	3.95	4.52	4.81
11.0 -	100.1	113.65	127.2
10.0 -	14.87	16.34	17.82
9.0 -	6.76	7.52	8.28
8.0 -	8.52	9.63	10.73
7.0 -	31.69	35.06	38.41
6.0 -	24.45	27.3	30.15
5.0 -	42.27	49.33	56.39
4.0 -	5.25	5.94	6.35
3.0 -	4.27	4.78	5.15
2.0 -	30.75	34.01	37.26
1.0 -	48.75	56.03	63.31
0.0 -	1.79	2.02	2.18

Figure 25. Energy requirements for desalination (GWh/yr) due to TDS content change in groundwater. This was calculated for Scenario 1 for each cluster

Cluster	TDS threshold to desalinate		
	500 (mg/l)	1000 (mg/l)	2000 (mg/l)
39.0 -	27.67	27.67	24.91
38.0 -	0.37	0.37	0.37
37.0 -	4.0	4.0	3.49
36.0 -	23.03	23.03	21.15
35.0 -	31.62	31.62	31.57
34.0 -	1.47	1.47	1.47
33.0 -	31.95	31.95	31.95
32.0 -	2.39	2.39	2.39
31.0 -	35.98	35.98	35.98
30.0 -	8.0	8.0	6.97
29.0 -	60.88	60.88	60.88
28.0 -	78.04	78.04	76.37
27.0 -	58.9	58.9	58.9
26.0 -	31.25	31.25	31.25
25.0 -	31.66	31.66	27.6
24.0 -	0.68	0.68	0.68
23.0 -	7.55	7.55	6.59
22.0 -	6.35	6.35	5.53
21.0 -	4.5	4.5	3.92
20.0 -	1.79	1.79	1.74
19.0 -	0.24	0.24	0.24
18.0 -	1.15	1.15	1.15
17.0 -	60.77	60.77	60.53
16.0 -	11.18	11.18	11.18
15.0 -	5.19	4.98	4.71
14.0 -	8.26	8.26	8.26
13.0 -	8.16	8.16	7.92
12.0 -	4.52	4.52	3.96
11.0 -	113.65	113.65	113.65
10.0 -	16.34	16.34	16.34
9.0 -	7.52	7.52	7.52
8.0 -	9.63	9.63	9.63
7.0 -	35.06	35.06	35.04
6.0 -	27.3	27.3	27.3
5.0 -	49.33	49.33	49.32
4.0 -	5.96	5.94	5.31
3.0 -	4.78	4.78	4.51
2.0 -	34.01	34.01	34.01
1.0 -	56.03	56.03	56.03
0.0 -	2.02	2.02	1.88

Figure 26. Energy requirements for desalination (GWh/yr) due to TDS threshold change to desalinate. This was calculated for Scenario 1 for each cluster

13.3. Irrigated area growth

For the sensitivity of irrigated area growth, three levels of growth in irrigated area were evaluated: low at 10%, medium at 20% and high at 40%. These values were chosen taking as basis the intensification rates presented in table 3, as if all in all region the intensification rate reaches 100%, the overall change in irrigated area would be circa 20%. Results are provided only for the overall aquifer. This is due to the fact that as the irrigated area was expanded, thus now the clustering algorithm may create different clusters. This makes some clusters to differ slightly between different growth scenarios. In general, irrigated area growth has important effects on total water withdrawals, total energy demand and total GWS, with increments of 25%, 23% and 23% respectively in the worst case (figures 27 to 29). It is important to mention, that these values are substantially improved by the reuse of treated wastewater/tailwater in irrigation.

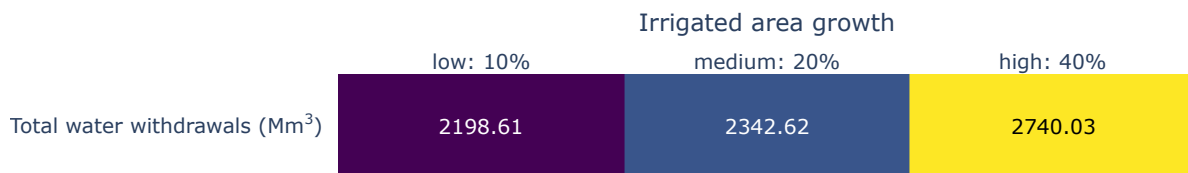


Figure 27. Total water withdrawals (Mm³/yr). This was calculated for Scenario 1 and all values were aggregated throughout the basin.

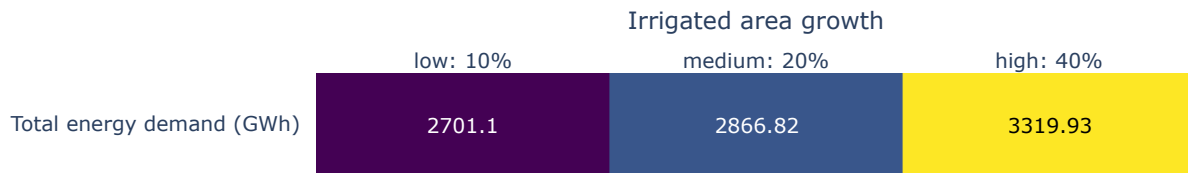


Figure 28. Total energy demand (GWh/yr). This was calculated for Scenario 1 and all values were aggregated throughout the basin.

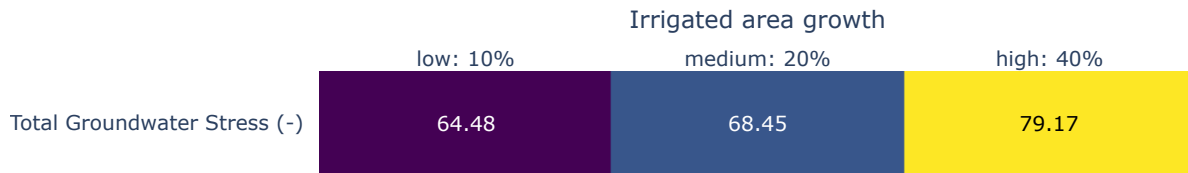


Figure 29. Total Groundwater Stress Indicator. This was calculated for Scenario 1 and all values were aggregated throughout the basin.

13.4. Population growth and domestic water use

The sensitivity of population growth and domestic water use per capita change, were evaluated by two levels of growth: low: 2% in Algeria and Libya and 1% in Tunisia [28], and medium: 3% in all countries. Moreover, three levels of domestic water use were accounted for based on ranges recommended by the World Health Organization to prevent health risks [13]. Outcomes show how domestic water use habits, seem to be more sensitive to the total water withdrawals and the associated energy requirements (figures 30-31 and 33-34). Moreover, it can be seen in figure 32 how the domestic water demand increases due to population growth and water use per capita, treatment systems fitted for larger treatment capacity as extended aeration are chosen.

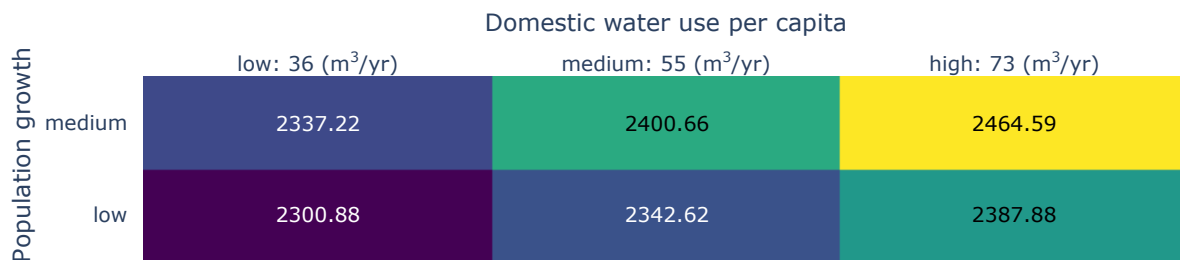


Figure 30. Total water withdrawals (Mm^3/yr) change due to population growth and domestic water usage. This was calculated for Scenario 1 and all values were aggregated throughout the basin.

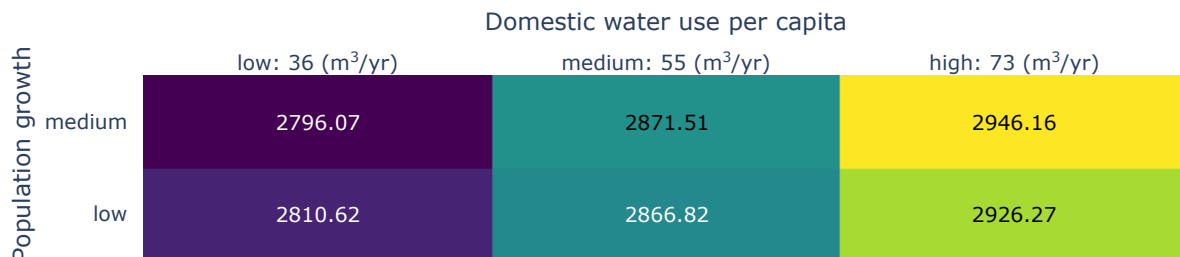


Figure 31. Total energy demand (GWh/yr) due to population growth and domestic water usage. This was calculated for Scenario 1 and all values were aggregated throughout the basin.

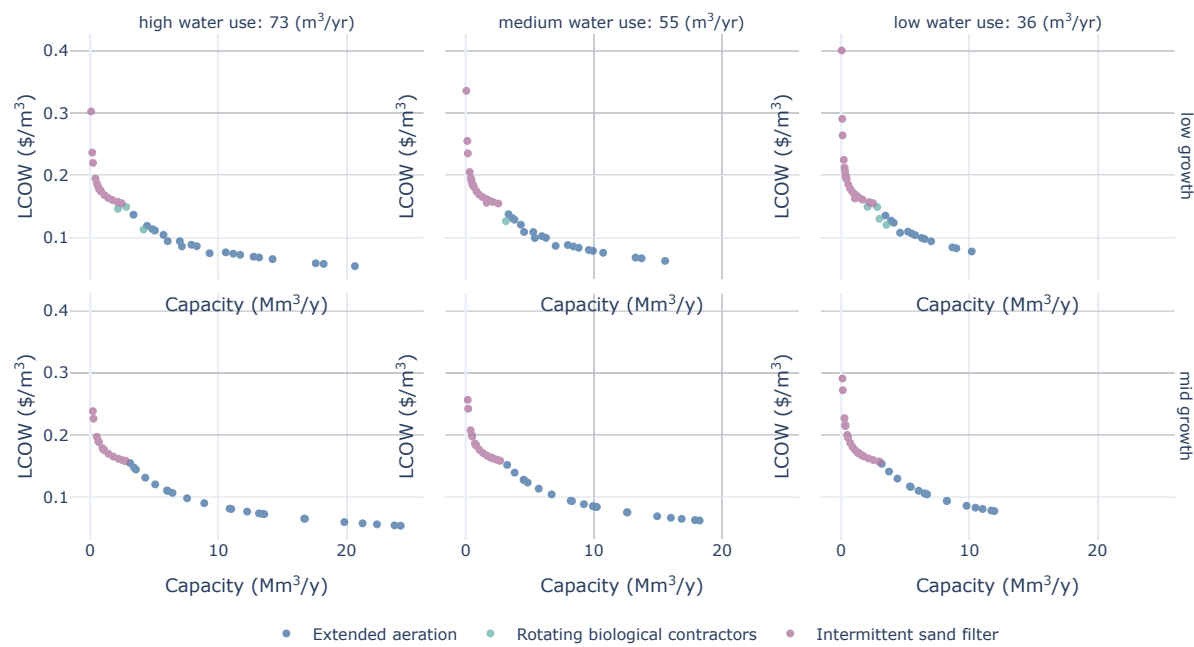


Figure 32. Sensitivity of Lest-cost domestic wastewater treatment technologies chosen to changes in population growth and water use per capita.

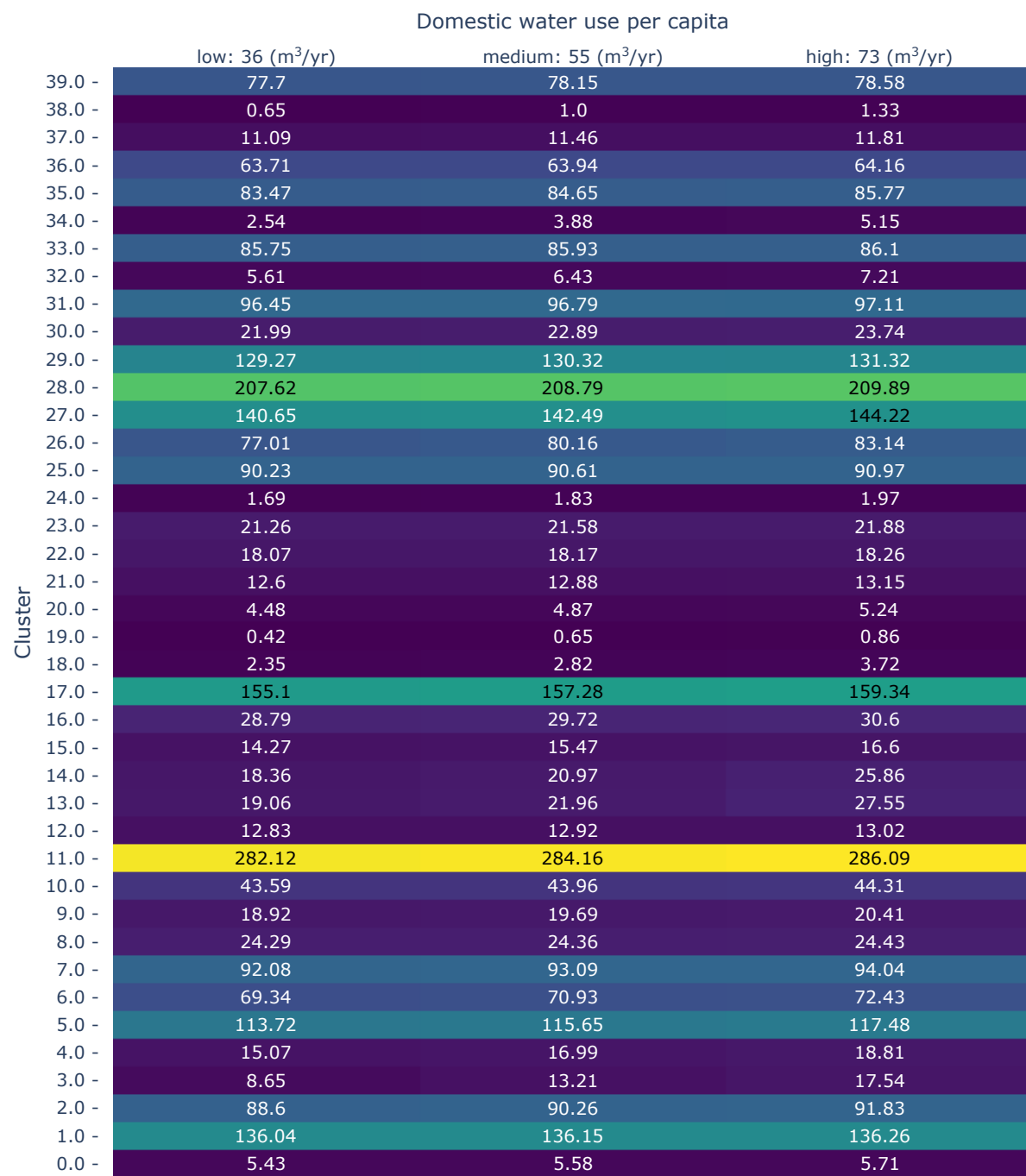


Figure 33. Total water withdrawals (Mm³/yr) change per cluster due to population growth and domestic water usage.

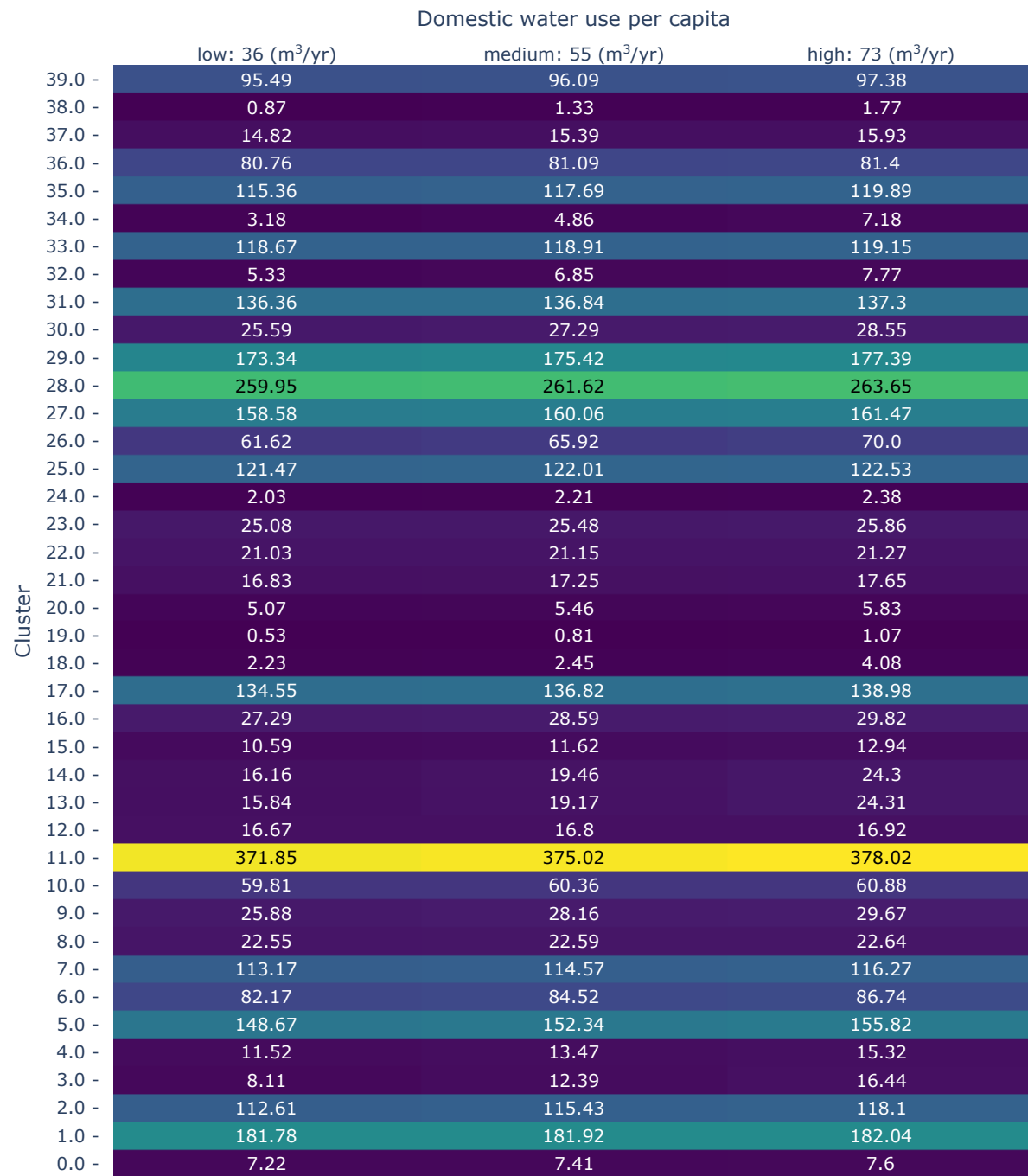


Figure 34. Total energy demand (GWh/yr) per cluster due to population growth and domestic water usage

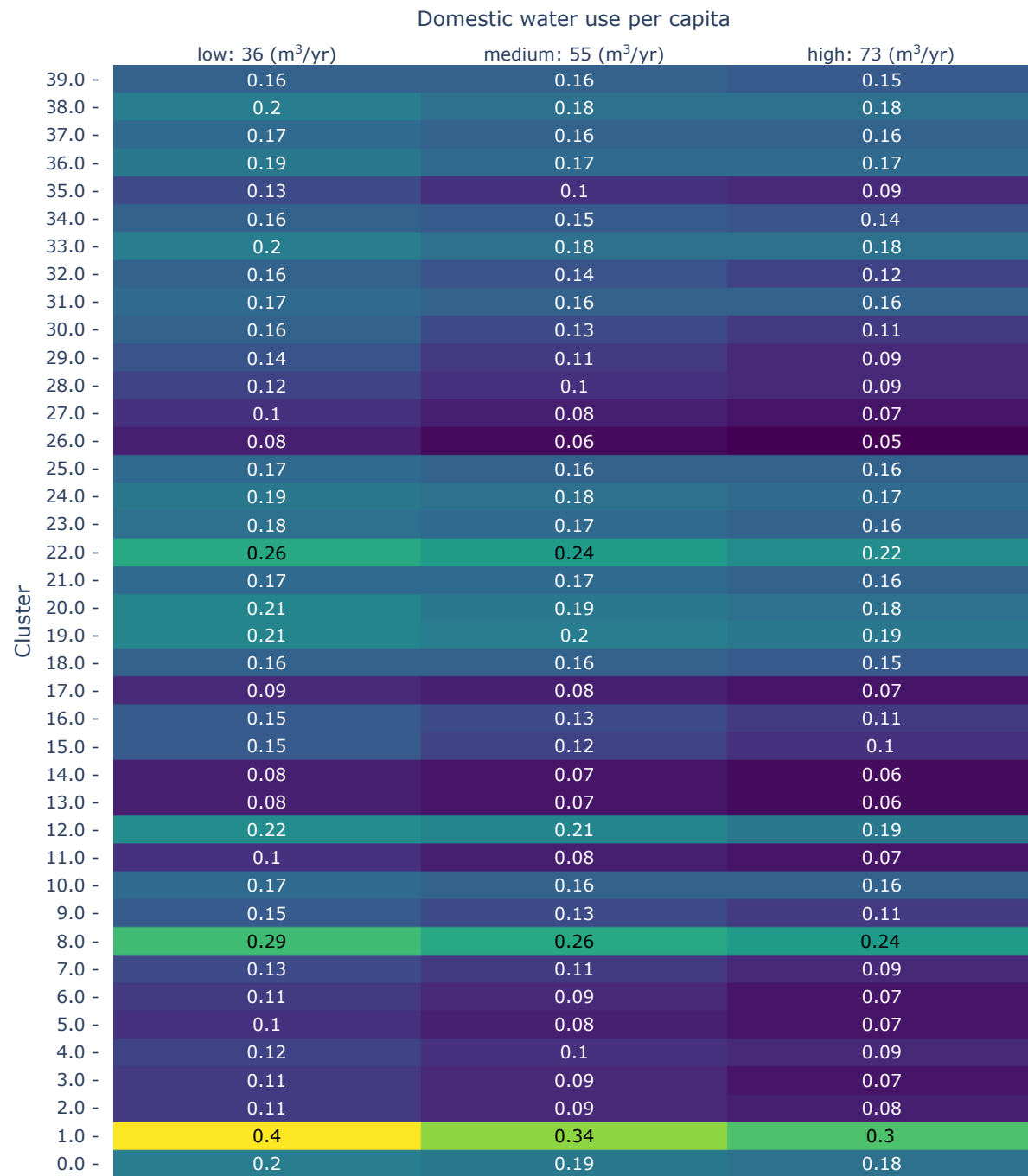


Figure 35. Sensitivity of LCOW (\$/m³) value of domestic wastewater treatment technologies chosen, to changes in population growth and water use per capita.

13.5. Discount rate

Finally, the sensitivity of the scenario analysis results to the discount rate was calculated. The paper uses a discount rate of 5%, which is higher than a social discount rate[‡] of 3% but lower than a typical business discount rate of 8%. As visible in figure 36 and figure 37 a different discount rate influence the leveled LCOW, however it does not change significantly the dynamics of the results (technologies chosen).



Figure 36. Average Levelized Cost of Water (LCOW) (\$/m³) calculated for different discount rates. The values average is reported for the NWSAS.

[‡] A Social Discount Rate is seen as a measure of a country's value of future costs and benefits, and is related to the notion of promoted sustainability.

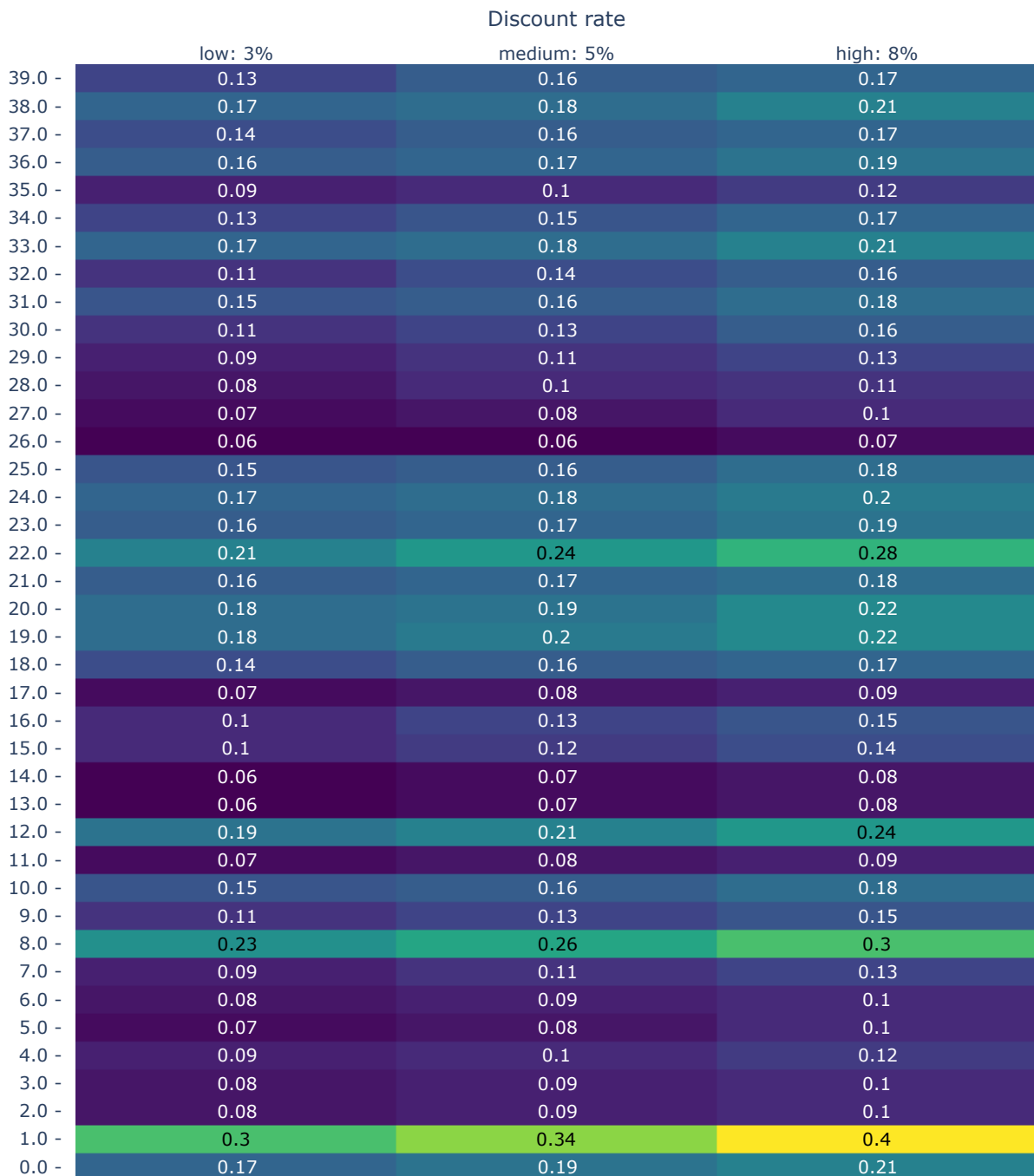


Figure 37. Levelized Cost of Water (LCOW) ($\$/\text{m}^3$) calculated for different discount rates. The values are reported for each cluster.

References

- [1] Catherine Linard, Marius Gilbert, Robert W. Snow, Abdisalan M. Noor, and Andrew J. Tatem. Population Distribution, Settlement Patterns and Accessibility across Africa in 2010. *PLOS ONE*, 7(2):1–8, 2012. doi: 10.1371/journal.pone.0031743.

- [2] OSS. *For a Better Valorization of Irrigation Water in the SASS Basin: Diagnosis and Recommendations*. Sahara and Sahel Observatory, 2015. ISBN 978-9973-856-87-6. NWSAS.
- [3] A M MacDonald, H C Bonsor, B É Ó Dochartaigh, and R G Taylor. Quantitative maps of groundwater resources in Africa. *Environmental Research Letters*, 7(2): 024009, 2012. ISSN 1748-9326. doi: 10.1088/1748-9326/7/2/024009.
- [4] GADM. Algeria, Tunisia and Libya country boundaries spatial data. <https://gadm.org/index.html>, 2018. Accessed: 2018-08-15.
- [5] IGRAC (International Groundwater Resources Assessment Centre). Transboundary Aquifers of the World [map]. Edition 2015. Scale 1 : 50 000 000. <https://gadm.org/index.html>, 2015. Accessed: 2018-08-15.
- [6] ESA Climate Change Initiative - Land Cover project. S2 prototype LC 20m map of Africa 2016. <http://2016africalandcover20m.esrin.esa.int/>, 2017. Accessed: 2018-08-15.
- [7] WorldClim - Global Climate Data. <http://www.worldclim.org/>, 2020.
- [8] Sahara and Sahel Observatory (OSS). Socio-economic aspects of irrigation in the SASS basin. A better water valorization for sustainable management of the basin. Technical report, Sahara and Sahel Observatory, 2014.
- [9] M. Chaouki, A. Zeddouri, and S. Hadj-Said. Study of the Behavior of Some Pollutants and the Vulnerability to Chemical Contamination of Groundwater in the Region of Ouargla (Southeast Algeria). *Energy Procedia*, 36:1043–1049, 2013. ISSN 1876-6102. doi: 10.1016/j.egypro.2013.07.119. URL <http://www.sciencedirect.com/science/article/pii/S1876610213012058>. TerraGreen 13 International Conference 2013 - Advancements in Renewable Energy and Clean Environment.
- [10] GeoData Institute, University of Southampton. Africa population count data, 2015. URL www.worldpop.org.
- [11] Youssef Almulla, Camilo Ramirez, Konstantinos Pegios, Alexandros Korkovelos, Lucia de strasser, Annukka Lipponen, and Mark Howells. A GIS-based approach to inform agriculture-water-energy nexus planning in the North Western Sahara Aquifer System (NWSAS). *Submitted to Sustainability*, Forthcoming.
- [12] Khaled AbuZeid, Mohamed Elrawady, and CEDARE. North Western Sahara Aquifer System (NWSAS) 2012 state of the Water Report. Technical report, Monitoring & Evaluation for Water in North Africa (MEWINA) project, Water Resource Management Program. CEDARE, 2015. Online.
- [13] Meriem Naimi-Ait-Aoudia and Ewa Berezowska-Azzag. Household water consumption in Algiers facing population growth. Water and Cities, Managing a Vital Relationship. *Proceedings of the 50th ISOCARP Congress, Urban Transformations, Cities and Water*, page 12, 9 2014.

- [14] Golam Saleh Ahmed Salem, So Kazama, Shamsuddin Shahid, and Nepal C. Dey. Groundwater-dependent irrigation costs and benefits for adaptation to global change. *Mitigation and Adaptation Strategies for Global Change*, 2017. ISSN 1573-1596. doi: 10.1007/s11027-017-9767-7. External.
- [15] Robert S Ayers and Dennis W Westcot. *Water quality for agriculture*, volume 29. Food and Agriculture Organization of the United Nations Rome, 1985.
- [16] M. Molinos-Senante, M. Garrido-Baserba, R. Reif, F. Hernández-Sancho, and M. Poch. Assessment of wastewater treatment plant design for small communities: Environmental and economic aspects. *Science of The Total Environment*, 427-428: 11–18, 2012. ISSN 00489697. doi: 10.1016/j.scitotenv.2012.04.023.
- [17] Pratima Singh, Cynthia Carliell-Marquet, and Arun Kansal. Energy pattern analysis of a wastewater treatment plant. *Applied Water Science*, 2(3):221–226, 2012. ISSN 2190-5495. doi: 10.1007/s13201-012-0040-7.
- [18] Renan Barroso Soares. Comparative Analysis of the Energy Consumption of Different Wastewater Treatment Plants. *International Journal of Architecture, Arts and Applications*, 3(6):79, 2017. ISSN 2472-1107. doi: 10.11648/j.ijaaa.20170306.11.
- [19] F. Hernández-Sancho, M. Molinos-Senante, and R. Sala-Garrido. Cost modelling for wastewater treatment processes. *Desalination*, 268(1):1–5, 2011. ISSN 0011-9164. doi: 10.1016/j.desal.2010.09.042.
- [20] A.K. Plappally and J.H. Lienhard V. Energy requirements for water production, treatment, end use, reclamation, and disposal. *Renewable and Sustainable Energy Reviews*, 16(7):4818–4848, 2012. ISSN 1364-0321. doi: 10.1016/j.rser.2012.05.022.
- [21] James A. Roumasset and Christopher Wada. Energy Costs and the Optimal Use of Groundwater. Allied Social Science Association (ASSA) Annual Meeting, January 3-5, 2014, Philadelphia, PA 161892, Agricultural and Applied Economics Association, 2013.
- [22] A. J. Karabelas, C. P. Koutsou, M. Kostoglou, and D. C. Sioutopoulos. Analysis of specific energy consumption in reverse osmosis desalination processes. 431: 15–21. ISSN 0011-9164. doi: 10.1016/j.desal.2017.04.006. URL <http://www.sciencedirect.com/science/article/pii/S0011916417302862>.
- [23] Shu-Yuan Pan, Andrew Z. Haddad, Arkadeep Kumar, and Sheng-Wei Wang. Brackish water desalination using reverse osmosis and capacitive deionization at the water-energy nexus. 183:116064. ISSN 0043-1354. doi: 10.1016/j.watres.2020.116064. URL <http://www.sciencedirect.com/science/article/pii/S0043135420306011>.
- [24] Ashlynn S. Stillwell and Michael E. Webber. Predicting the Specific Energy Consumption of Reverse Osmosis Desalination. *Water*, 8(12):601, December 2016. ISSN 2073-4441. doi: 10.3390/w8120601. WOS:000392480200054.

- [25] S. Aminfard, F.T. Davidson, and M.E. Webber. Multi-layered spatial methodology for assessing the technical and economic viability of using renewable energy to power brackish groundwater desalination. *Desalination*, 450:12–20, January 2019. ISSN 00119164. doi: 10.1016/j.desal.2018.10.014.
- [26] John C. Crittenden, R. Rhodes Trussell, David W. Hand, Kerry J. Howe, and George Tchobanoglous. *MWH's Water Treatment: Principles and Design*. John Wiley & Sons, Inc., 2012. ISBN 978-1-118-13147-3 978-0-470-40539-0. doi: 10.1002/9781118131473.
- [27] Stefan Reichelstein and Michael Yorston. The prospects for cost competitive solar PV power. *Special section: Long Run Transitions to Sustainable Economic Structures in the European Union and Beyond*, 55:117–127, 2013. ISSN 0301-4215. doi: 10.1016/j.enpol.2012.11.003.
- [28] UNECE. Reconciling resource uses: Assessment of the water-food-energy-ecosystems nexus in the North Western Sahara Aquifer System, Part A - "Nexus Challenges and Solutions. URL <http://www.unece.org/index.php?id=55154>.